



1 **Wildfires in Northern Eurasia affect the budget of black**
2 **carbon in the Arctic. A 12-year retrospective synopsis**
3 **(2002–2013).**

4
5 **N. Evangeliou**^{1,2*}, **Y. Balkanski**¹, **W. M. Hao**³, **A. Petkov**³, **R. P. Silverstein**³, **R.**
6 **Corley**³, **B. L. Nordgren**³, **S. P. Urbanski**³, **S. Eckhardt**², **A. Stohl**², **P. Tunved**⁴,
7 **S. Crepinsek**^{5,6}, **A. Jefferson**⁶, **S. Sharma**⁷, **J. K. Nøjgaard**⁸, **H. Skov**⁸

- 8
9 [1] CEA-UVSQ-CNRS UMR 8212, Laboratoire des Sciences du Climat et de
10 l'Environnement (LSCE), Institut Pierre et Simon Laplace, L'Orme des Merisiers, F-91191
11 Gif sur Yvette Cedex, France.
12 [2] Norwegian Institute for Air Research (NILU), Department of Atmospheric and Climate
13 Research (ATMOS), Kjeller, Norway.
14 [3] Missoula Fire Sciences Laboratory, Rocky Mountain Research Station, United States
15 Forest Service, Missoula, Montana, USA.
16 [4] Department of Applied Environmental Science, Stockholm University, Stockholm,
17 Sweden
18 [5] Cooperative Institute for Research in Environmental Sciences, University of Colorado,
19 Boulder, Colorado, USA.
20 [6] NOAA Earth System Research Laboratory Physical Sciences Division/Polar Observations
21 & Processes, Boulder, Colorado, USA.
22 [7] Climate Research Division, S&T Branch, Environment Canada, Toronto, Ontario,
23 Canada.
24 [8] Department of Environmental Science, Aarhus University, DK-4000 Roskilde, Denmark.

25
26 Correspondence to: N. Evangeliou (Nikolaos.Evangeliou@nilu.no)
27



1 **Abstract**

2 In recent decades much attention has been given to the Arctic environment, where climate
3 change is happening rapidly. Black carbon (BC) has been shown to be a major component of
4 Arctic pollution that also affects the radiative balance. In the present study, we focused on
5 how vegetation fires that occurred in Northern Eurasia during the period of 2002–2013
6 influenced the budget of BC in the Arctic. For simulating the transport of fire emissions from
7 Northern Eurasia to the Arctic, we adopted BC fire emission estimates developed
8 independently by GFED3 (Global Fire Emissions Database) and FEI-NE (Fire Emission
9 Inventory - Northern Eurasia). Both datasets were based on fire locations and burned areas
10 detected by MODIS (MODerate resolution Imaging Spectroradiometer) instruments on
11 NASA's (National Aeronautics and Space Administration) Terra and Aqua satellites.
12 Anthropogenic sources of BC were estimated using the MACCity (Monitoring Atmospheric
13 Composition & Climate / megaCITY - Zoom for the ENvironment) emission inventory.

14 During the 12-year period, an average area of $250,000 \text{ km}^2 \text{ yr}^{-1}$ was burned in Northern
15 Eurasia and the global emissions of BC ranged between 8.0 and 9.5 Tg yr^{-1} . For the BC
16 emitted in the Northern Hemisphere, about 70% originated from anthropogenic sources and
17 the rest from biomass burning (BB). Using the FEI-NE inventory, we found that $102 \pm 29 \text{ kt yr}^{-1}$
18 BC from biomass burning was deposited on the Arctic (defined here as the area north of
19 67°N) during the 12 years simulated, which was twice as much as when using MACCity
20 inventory ($56 \pm 8 \text{ kt yr}^{-1}$). The annual mass of BC deposited in the Arctic from all sources
21 (FEI-NE in Northern Eurasia, MACCity elsewhere) is significantly higher by about 37% in
22 2009 to 181% in 2012, compared to the BC deposited using just the MACCity emission
23 inventory. Deposition of BC in the Arctic from BB sources in the Northern Hemisphere thus
24 represents 68% of the BC deposited from all BC sources (the remaining being due to
25 anthropogenic sources). Northern Eurasian vegetation fires (FEI-NE) contributed 85% (79–
26 91%) to the BC deposited over the Arctic from all BB sources in the Northern Hemisphere.
27 Arctic total BC burden showed strong seasonal variations, with highest values during the
28 Arctic Haze season. High winter–spring values of BC burden were caused by transport of BC
29 mainly from anthropogenic sources in Europe, whereas the peak in summer was mainly due
30 to the fire emissions in Northern Eurasia. BC particles emitted from fires in lower latitudes
31 (35°N – 40°N) were found to remain the longest in the atmosphere due to the high release
32 altitudes of smoke plumes, exhibit tropospheric transport resulting in a high summer peak of
33 burden, and grow by condensation processes.



1 In regards to the geographic contribution on the deposition of BC, we estimated that
2 about 46% of the BC deposited over the Arctic from vegetation fires in Northern Eurasia
3 originated from Siberia, 6% from Kazakhstan, 5% from Europe, and about 1% from
4 Mongolia. The remaining 42% originated from other areas in Northern Eurasia. For spring
5 and summer, we computed that 42% of the BC released from Northern Eurasian vegetation
6 fires was deposited over the Arctic (annual average: 17%). Vegetation fires in Northern
7 Eurasia contributed to 14% to 57% of BC surface concentrations at the Arctic stations (Alert,
8 Barrow, Zeppelin, Villum, and Tiksi), with fires in Siberia contributing the largest share.
9 However, anthropogenic sources in the Northern Hemisphere remain essential, contributing
10 29% to 54% to the surface concentrations at the Arctic monitoring stations. The rest
11 originated from North American fires.
12



1 **1 Introduction**

2 The Arctic environment has experienced rapid modifications (e.g. warming, ice
3 degradations, etc.) during the last four decades and concerns have been raised that human
4 activities were the main cause for these transformations. The thinning of Arctic sea ice
5 (Hansen and Nazarenko, 2004) and the Arctic's rapidly growing human influence (e.g.
6 transportation, drilling, industry) indicates the need not only for further decrease of
7 greenhouse emissions, but also a better understanding of aerosol properties, as well as of
8 aerosol interaction with radiation, clouds, and ecosystems in Polar Regions. The "Arctic
9 Haze" phenomenon in winter and spring is a major feature of Arctic air pollution. Several
10 studies have been conducted to determine the sources of Arctic air pollution using trajectory,
11 regional, and global models (e.g., Hirdman et al., 2010a; Klonecki et al., 2003; Koch and
12 Hansen, 2005; Law and Stohl, 2007; Stohl, 2006). They all agree that the majority of the
13 pollution in the high-latitude Arctic, especially near the surface, originates at mid- and high-
14 latitudes, and that the accumulation of pollution in the Arctic is a consequence of the slow
15 removal processes in winter and spring (Shaw, 1995). Also, Northern Eurasia (Europe,
16 Siberia, Kazakhstan, Mongolia, etc.) is the main source of the Arctic BC due to both wildfire
17 and anthropogenic emissions.

18 Episodic emissions from mid- and high-latitude vegetation fires can affect tropospheric
19 concentrations of trace gases (e.g. carbon monoxide (CO), ozone (O₃), volatile organic
20 compounds (VOC), and aerosols (e.g. BC)) several thousand kilometers away from the
21 sources (Forster et al., 2001; Wotawa and Trainer, 2000). Additionally, emissions from boreal
22 fires lifted by convection can substantially alter upper tropospheric and the lowermost
23 stratospheric radiation balance and chemistry (Waibel et al., 1999; Jost et al., 2004; Fromm et
24 al., 2005). Aerosols and trace gases are uplifted during transport to the Arctic due to the
25 upward sloping surfaces of constant potential temperature towards the Arctic (Klonecki et al.,
26 2003; Stohl, 2006). However, understanding of aerosol transport from mid-latitudes to the
27 Arctic has been limited because of the lack of quantification of the relevant aerosol sources
28 and removal processes.

29 Globally, BC contributed to climate warming with recent estimates of radiative forcing
30 at the top of the atmosphere ranging between 0.17 and 0.71 W m⁻² (Bond et al., 2013; Myhre
31 et al., 2013; Wang et al., 2014). Snow albedo may be reduced by 1–3% in fresh snow by BC
32 deposited in the Arctic and by another factor of 3 as snow ages and the BC becomes more
33 concentrated (Clarke and Noone, 1985). Hansen and Nazarenko (2004) found that the
34 decreased albedo in Arctic snow and ice since preindustrial times resulted in a hemispheric



1 radiative forcing of $+0.3 \text{ W m}^{-2}$, which may have had a substantial impact on the climate in
2 the Northern Hemisphere, while for Northern Russia it amounts to 0.2 W m^{-2} (Lee et al.,
3 2013a; 2013b). Airborne soot also absorbs incoming solar radiation thus warming the air and
4 reducing tropical cloudiness (Ackerman et al., 2000).

5 Biomass burning (BB) constitutes a major source of BC, in addition to incomplete
6 combustion of fossil fuels (primarily coal and diesel) and burning of biofuels. BC is the most
7 absorbing portion of carbonaceous aerosols, commonly referred to as “soot”. Vegetation fires,
8 either anthropogenic or natural, constitute a major source of atmospheric BC concentrations.
9 BC deposited on snow/ice surfaces reduces surface reflectance and can promote faster melting
10 of snow/ice in the Arctic, which is tightly coupled to climate effects through snow-albedo
11 feedback (Flanner et al., 2007, 2009; Hansen and Nazarenko, 2004). In addition, high aerosol
12 concentrations in the Arctic Haze lead to the enhancement of cloud longwave emissivity
13 (Garrett and Zhao, 2006; Lubin and Vogelmann, 2006), leading to surface warming and
14 accelerating the melting of snow/ice.

15 Model simulations by Stohl (2006) suggested that the contributions from BB to Arctic
16 BC loadings, particularly from fires in Siberia, exceeded the anthropogenic contributions in
17 the summer. Moreover, large amounts of BC from Siberia and Kazakhstan have been
18 observed during aircraft campaigns over Alaska in spring 2008 (Warneke et al., 2009), which
19 was a year with an unusually early start of the BB season in Northern Eurasia. Warneke et al.
20 (2010) estimated that BB in Russia may have doubled aerosol concentrations in the Arctic
21 Haze during the spring. BC has been monitored at several surface stations in the Arctic (e.g.
22 Alert in Canada, Barrow in Alaska, and Janiskoski in Russia) for many years (e.g. Sirois and
23 Barrie, 1999; Sharma et al., 2006; Quinn et al., 2008; Eleftheriadis et al., 2009; Gong et al.,
24 2010; Huang et al., 2010 and many others), showing decreasing trends during the 1980s and
25 1990s, which have been attributed to reductions in anthropogenic emissions (Sharma et al.,
26 2013; Hirdman et al., 2010b).

27 In this study, we focused on the transport of BC produced by vegetation fires in
28 Northern Eurasia to the Arctic from 2002 to 2013. We define Northern Eurasia from 10°W to
29 170°E and 35°N to 80°N . The Arctic is defined here as the area north of the Arctic Circle
30 ($\sim 67^{\circ}\text{N}$). Fires were mapped using satellite measurements from MODIS on NASA’s Terra
31 and Aqua satellites. We investigated the geographic distribution of BC sources contributing to
32 the Arctic BC budget, which needed to be better understood for developing BC mitigation
33 policies. Moreover, the transport of BC to the Arctic after vegetation fires was defined as
34 transport efficiency of BC. Shindell et al. (2008) showed large differences in the calculated



1 BC concentrations in the Arctic using different General Circulation Models (GCMs). A large
2 part of these differences was attributed to the different model treatment of BC aging from
3 hydrophobic to hydrophilic and rainout/washout processes during transport. It indicated the
4 necessity of a continuously improving description of BC transport in order to better assess the
5 impact on the Arctic climate despite many recent improvements (e.g. Browse et al., 2012;
6 Eckhardt et al., 2015).

7 This paper consists of five sections. The methodology (transport model, model set-up,
8 emission altitude, satellite-derived BC emissions) is discussed in detail in the next section.
9 The results, with respect to Arctic transport and deposition of BC, are presented in Section 3.
10 Then, we show how different regions in Northern Eurasia contribute to the Arctic BC,
11 distinguishing between anthropogenic and BB sources (Section 3.3). In Section 4.1, we
12 discuss how our modeling results compare to observations of BC using data from five
13 different Arctic stations for the period of our simulations (2002–2013). Finally, we calculate
14 and study transport efficiencies of BC to the Arctic from different BB regions (Section 4.2).
15 The main conclusions are presented in Section 5.

16 **2 Methodology**

17 **2.1 The LMDz-OR-INCA model**

18 We used the LMDz-OR-INCA global chemistry-aerosol-climate model, which couples
19 the LMDz (Laboratoire de Météorologie Dynamique) GCM (Hourdin et al., 2006) and the
20 INCA (INteraction with Chemistry and Aerosols) model (Hauglustaine et al., 2004). The
21 interaction between the atmosphere and the land surface was ensured through the coupling of
22 LMDz with the ORCHIDEE (ORganizing Carbon and Hydrology In Dynamic Ecosystems)
23 dynamical vegetation model (Krinner et al., 2005). In the present configuration, the model
24 included 39 hybrid vertical levels extending to the stratosphere, and a horizontal resolution of
25 $1.29^{\circ} \times 0.94^{\circ}$ (280 grid-cells in longitude, 192 in latitude). A more detailed description and an
26 extended evaluation of the GCM can be found in Hourdin et al. (2006). The large-scale
27 advection of tracers was calculated based on a monotonic finite-volume second-order scheme
28 (Hourdin and Armengaud, 1999). Deep convection was parameterized according to the
29 scheme of Emanuel (1991). The turbulent mixing in the planetary boundary layer (PBL) was
30 based on a local second-order closure formalism. A comparison made with inert tracers
31 indicated an enhanced vertical transport as the horizontal resolution of the model was
32 increased from 144×142 grid-points to 280×192 .



1 The INCA model simulates the distribution of anthropogenic aerosols such as sulfates,
2 nitrate (NO₃), BC, particulate organic matter (POM), as well as natural aerosols such as sea-
3 salt and dust. The aerosol model keeps track of both the number and the mass of aerosols
4 using a modal approach to treat the size distribution, which is described by a superposition of
5 5 log-normal modes (Schulz, 2007), each with a fixed spread. To treat the optically relevant
6 aerosol size diversity, particle modes were categorized in three ranges: sub-micronic
7 (diameter < 1 μm) corresponding to the accumulation mode, micronic (diameter 1–10 μm)
8 corresponding to coarse particles, and super-micronic or super coarse particles (diameter > 10
9 μm). Compared to a bin-scheme, the treatment of the size distribution with modes was
10 computationally much more efficient (Schulz et al., 1998). Furthermore, to account for the
11 diversity in chemical composition, hygroscopicity, and mixing state, we distinguished
12 between soluble and insoluble modes. In both sub-micron and micron size ranges, soluble and
13 insoluble aerosols were treated separately. Sea-salt, SO₄, and methane sulfonic acid (MSA)
14 were treated as soluble components of the aerosol, dust was treated as insoluble, whereas
15 nitrate, BC, and POM appeared both in the soluble and insoluble fractions. The aging of
16 primary insoluble carbonaceous particles transfers insoluble aerosol number and mass to
17 soluble ones with a half-life of 1.1 days (Chung et al., 2002). The deposition scheme used in
18 the model is described in detail in Evangeliou et al. (2013).

19 **2.2 Model set-up, BC inventories and injection height**

20 The simulations lasted from January 1st, 2002 to December 31st, 2013. The model ran in
21 a nudged mode using 6-hourly ERA Interim Re-analysis data (ECMWF, 2014) with a
22 relaxation time of 10 days (Hourdin and Issartel, 2000).

23 To support the IPCC-AR5 (Intergovernmental Panel for Climate Change Assessment
24 Report 5) and the ACCMIP (Atmospheric Chemistry and Climate - Model Intercomparison
25 Project), a historical emissions dataset was developed (Lamarque et al, 2010) on a decadal
26 basis (from 1850 to 2000 for the historical dataset), as well as RCP (Representation
27 Concentration Pathways) emission scenarios for the period after the year 2000. As part of a
28 project funded by the European Commission, MACC (Monitoring Atmospheric Composition
29 & Climate) and CityZen (megaCITY - Zoom for the ENvironment), the ACCMIP and the
30 RCP emissions dataset were adapted and extended to the year 2013 on a yearly basis. For
31 anthropogenic emissions, emission data was interpolated on a yearly basis. For BB emissions,
32 the ACCMIP dataset was extended to yearly and monthly mean calculated from modified
33 RETRO (REanalysis of the TROposhperic chemical composition) BC emission data for the



1 years 1980 to 1996, and from GFEDv3 carbon emission data for the years 1997 to 2013, by
2 applying a single set of vegetation type specific emission factors, and the predominant
3 vegetation map used in the GFEDv3 inventory. This extension of the ACCMIP and RCP
4 emission dataset for the MACC and CityZEN projects is referred to as MACCity
5 (MACC/CityZen) emission dataset (Granier et al., 2011). As it is explained below, emissions
6 of MACCity (anthropogenic and BB) were used as the input source of the model worldwide,
7 in which BB sources were derived from GFEDv3. In addition, we adopted BC emissions from
8 BB in Northern Eurasia from 2002 to 2013 (FEI-NE) described in the companion paper (Hao
9 et al., 2015), while MACCity emissions were used for all the sources in other regions and for
10 anthropogenic sources in Northern Eurasia.

11 Injection height is a key factor that controls transport and in turn deposition of BC
12 emitted from fires. It is generally accepted that only explosive volcanic eruptions and strong
13 crown fires (more common in North America than in Northern Eurasia) have the energy to
14 inject pollutants from the surface into the stratosphere (Jost et al., 2004; Fromm et al., 2005).
15 In a modeling study of mid-latitude supercell thunderstorms (Wang, 2003), it was reported
16 that these plumes could induce important transport into the lowermost stratosphere. These
17 findings suggest that extreme convection, even unassociated with energetic forest fires, may
18 represent an important pathway for rapid, efficient redistribution of gases and particles from
19 the lowest levels of the atmosphere to the lower stratosphere or, more commonly, the upper
20 troposphere. Nedelec et al. (2005) described such a case for a fire happening over Siberia.
21 However, injection of emissions in the lower troposphere is more common. Recently, Sofiev
22 et al. (2013) published global maps of emission heights of wildfires that occurred between
23 2000 and 2012 reporting that about 80% of the smoke is generally injected within the PBL,
24 while the rest is injected at higher altitudes. Here we follow the same pattern as Sofiev et al.
25 (2013) for Northern Eurasia, where 90% of the emissions were injected below 1.1 km, while
26 the rest in heights up to 1.5 km.

27 **2.3 BC emissions from FEI-NE and MACCity**

28 For the 12-year global simulations, anthropogenic sources of BC were adopted from the
29 MACCity emission database. As regards to BB emissions, MACCity BB emissions from
30 GFED3 were applied for all the regions outside Northern Eurasia, while within Northern
31 Eurasia anthropogenic emissions from MACCity and BB from FEI-NE (Hao et al., 2015)
32 were adopted. In summary, BC emissions from BB, excluding agricultural fires, in Northern



1 Eurasia were estimated based on the area burned, fuel loading, percentage of the fuel burned,
2 and emission factors of BC from different vegetation types (Hao et al., 2015).

3 This combined simulation is hereafter referred to as FEI-NE+MACCcity. For
4 comparison, we carried out the same simulation but using MACCcity emissions alone (i.e. BB
5 emissions in Northern Eurasia were also taken from MACCcity) for the same period (2002–
6 2013) (from now on referred to it as MACCcity simulation). The different simulations are
7 shown in Table 1.

8 2.4 Lifetime calculations

9 Several definitions for atmospheric lifetime exist. In any domain of Earth's atmosphere
10 the mass balance can be expressed as:

$$11 \quad \frac{dB(t)}{dt} = S(t) - \frac{B(t)}{\tau(t)} \quad (\text{Eq. 1})$$

12 where $B(t)$ is the atmospheric burden, $S(t)$ is the mass entering or exiting the domain and
13 $\tau(t)$ is the removal time over a given time-step. If one assumes equilibrium between $S(t)$ and
14 deposition (steady state conditions), the mean steady state lifetime will be:

$$15 \quad \tau_{ss} = \frac{\bar{B}}{\bar{D}} \quad (\text{Eq. 2})$$

16 where \bar{B} and \bar{D} are the mean atmospheric burden and deposition over a specific period (Croft
17 et al., 2014).

18 2.5 Observation data

19 With different types of instruments, we collected measurements of BC, which may not
20 always be directly comparable. Following the nomenclature of Petzold et al. (2013), we
21 referred to measurements based on light absorption as equivalent BC (eBC) and
22 measurements based on thermal-optical methods as elemental carbon (EC).

23 Aerosol light absorption data was obtained from five sites in different parts of the
24 Arctic: Alert, Canada (62.3°W, 82.5°N; 210 m above sea level (a.s.l.)), Barrow, Alaska
25 (156.6°W, 71.3°N; 11 m a.s.l.), Zeppelin/Ny Ålesund, Spitsbergen, Norway (11.9°E, 78.9°N;
26 478 m a.s.l.), and Tiksi, Russia (128.9°E, 15 71.6°N; 1 m a.s.l.). Different types of particle
27 soot absorption photometers (PSAPs) were used for the measurements at Barrow and
28 Zeppelin, and an aethalometer was used at Alert and Tiksi. All these instruments measured
29 the particle light absorption coefficient σ_{ap} , each at its own specific wavelength (typically at
30 around 530–550 nm), and for different size fractions of the aerosol (typically particles smaller
31 than 1, 2.5, or 10 μm are sampled at different humidities). Conversion of σ_{ap} to eBC mass



1 concentrations is not straightforward and requires certain assumptions (Petzold et al., 2013).
2 The mass absorption efficiency used for conversion can be specific to a site and is uncertain
3 by at least a factor of two. For Tiksi, the conversion was done internally by the aethalometer.
4 For the other sites, a mass absorption efficiency of $10 \text{ m}^2 \text{ g}^{-1}$, typical of aged BC aerosol
5 (Bond and Bergstrom, 2006), was used. Sharma et al. (2013) used an even higher value of 19
6 $\text{m}^2 \text{ g}^{-1}$ for Barrow and $10 \text{ m}^2 \text{ g}^{-1}$ for Alert data.

7 At Villum Research Station, Station Nord, Greenland, thermo-optical measurements
8 were available. Weekly aerosol samples were analyzed with a thermal-optical Lab OC/EC
9 instrument from Sunset Laboratory Inc (Tigard, OR, USA). Punches of 2.5 cm^2 were cut from
10 the filters sampled at Villum and analyzed according to the EUSAAR-2 protocol (Cavalli et
11 al., 2010).

12 At Alert, eBC data was available for the years 2006–2013, at Barrow for 2002–2013, at
13 Tiksi for 2009–2013, and at Zeppelin for 2002–2013. At Villum station, EC data was
14 available for 2008–2011. The EC and eBC data were directly compared with modeled BC
15 concentrations for the same locations and periods. Tiksi data was not filtered for a clean air
16 sector and may have been affected by local pollution events. Barrow and Alert data were
17 routinely subject to data cleaning, which removed the influence from local sources. Zeppelin
18 generally was not strongly influenced by local emissions; however, summer values were
19 enhanced by some 11% due to local cruise ship emissions (Eckhardt et al., 2013).

20 **3 Results**

21 **3.1 Emission, transport and deposition of BC**

22 Northern Eurasia encompasses diverse ecosystems including forest, shrubland,
23 cropland, grassland, and savanna (Friedl et al., 2002). The total burned areas (excluding
24 agricultural fires) during the period of 2002–2013 were estimated to be $250,000 \text{ km}^2 \text{ yr}^{-1}$ ($n =$
25 12) (Hao et al., 2015), which consisted of 61% of grassland and 27% of forest. Grassland fires
26 occurred predominantly over Central and Western Asia, and forest fires over Siberia in
27 Russia. The years 2003, 2006, and 2008 showed 96%, 40%, and 30%, respectively, more fire
28 detections than the annual mean from 2002 to 2013 (Figure S 1). The unusual high fire
29 activity in 2003, 2006, and 2008 was a result of extensive grassland fires over Central and
30 Western Asia, and forest and grassland fires over Russia.

31



1 Table 2 presents the yearly mean atmospheric emissions of BC from anthropogenic and
2 BB sources for the period 2002–2013 from the FEI-NE+MACCity and the MACCity
3 simulation. Annual global BC emissions varied in a range from 8.02 Tg in 2007 to 9.48 Tg in
4 2003 with an average: 8.42 ± 0.43 Tg yr⁻¹ over the period 2002 to 2013 according to FEI-NE
5 and MACCity. These values compared well with other published results. For instance, Wang
6 et al. (2014) reported that, according to PKU-BC-2007 (Peking University BC Inventory for
7 2007) inventory of global BC emissions (both anthropogenic and biomass burning sources), a
8 total amount of 8.9 Tg was emitted in 2007. The ECLIPSE inventory estimated for 2010 by
9 Eckhardt et al. (2015) was 8.32 Tg, only slightly higher than our estimations of 8.02 Tg. In
10 contrast, the ACCMIP BC emissions for 2005 (Lamarque et al., 2010) was 15% lower (e.g.
11 ~7.82 Tg compared to 8.13 Tg). BC emissions from vegetation fires in Northern Eurasia
12 ranged between 0.45 and 2.19 Tg for the period 2002–2013 representing 20% to 49% of the
13 total BC emissions over this region. In comparison, the emissions over the same region based
14 on the MACCity inventory ranged between 0.13 and 0.43 Tg and accounted for 5% to 16% of
15 total BC emissions. The BC emissions in the Northern Hemisphere (FEI-NE+MACCity) were
16 classified as 70% from anthropogenic sources and 30% from BB. Northern Eurasian
17 vegetation fires accounted for 56% of the BB BC emissions in the Northern Hemisphere
18 (Bond et al., 2013).

19 BC emissions from FEI-NE were relatively constant in time except for four intense
20 years (Figure S 2). Similarly, the GFED3 of MACCity showed relatively high emissions in
21 some of these years (2003 and 2006), but the relative emission increase was significantly
22 lower for these years (Table 2). The fire episodes that occurred in Northern Eurasia during
23 these extreme fire years were particularly intense. In 2003, fire events in the Transbaikal
24 region (Russian provinces Chita and Buryatia) caused severe smoke pollution in the Far East
25 of the Russian Federation (IFFN, 2004), while in spring 2006, smoke from peat and forest
26 fires in the western Russian Federation was noted as far as the United Kingdom (Hao et al.,
27 2009) and in the Arctic (Stohl et al., 2007). In summer 2006, smoke from vegetation fires in
28 the Russian Federation persisted for weeks over Finland (GFMC, 2006).

29 Figure 1 depicts deposition anomalies of BC for the period 2002–2013. A remarkable
30 feature was that the highest anomalies were observed in the northernmost part of Asia and the
31 Arctic in 2003, 2006, 2008, and 2012. This indicates that during these years the largest
32 amounts of BC were deposited over Arctic regions as a result of large fire events in Siberia,
33 Western Russia, and Kazakhstan. The annual amount of BC deposited over the Arctic from
34 all possible global sources (including BB) during the 12-year period ranged from 65 kt to 152



1 kt (average: 102 ± 29 kt yr⁻¹) representing about 0.9–18% of total global emissions. The total
2 annual deposition of BC to the Arctic from vegetation fires in Northern Eurasia (FEI-NE)
3 during the same period ranged between 29–120 kt (average: 65 ± 28 kt yr⁻¹) or about 0.3–14%
4 of total global BB emissions (Table 2). Hence, more than half of the total BC that deposited
5 over the Arctic originated from BB in Northern Eurasia and underlined the importance of the
6 Northern Eurasian vegetation fires on the Arctic BC budget, on par with the contribution of
7 other sources.

8 Figure 2 illustrates BC deposition from FEI-NE detected vegetation fires only,
9 excluding anthropogenic sources, while Figure S 3 shows the deposition from all sources
10 (FEI-NE+MACCcity). For the most intense fire years, 2003, 2006, 2008, and 2012, an annual
11 amount of 142, 129, 117, and 152 kt of BC, respectively, was deposited over the Arctic from
12 Northern Eurasian vegetation fires (Table 2). It amounts to 3.2 to 4.1 times the 37 ± 5 kt yr⁻¹
13 average (2002 to 2013) deposition flux for anthropogenic sources over Northern Eurasia.
14 Finally, when using MACCcity emissions, both from anthropogenic and BB sources, the
15 estimated average deposition of BC over the Arctic was 56 ± 8 kt yr⁻¹ for the period 2002–
16 2013. Consequently, Arctic deposition was lower by 45% compared to FEI-NE, when BB
17 emissions of BC from GFED (MACCcity) were used.

18 3.2 Aerosol lifetime and seasonality of BC

19 Figure 3 depicts the global mean aerosol lifetimes for anthropogenic and BB BC from
20 the combined FEI-NE+MACCcity simulation. The results are given in Box & Whisker plots of
21 daily lifetimes for the 12-year period. Mean aerosol lifetimes for anthropogenic BC were
22 stable for all the studied years with an annual average value of 5.6 ± 0.2 d. Mean aerosol
23 lifetimes of BC from FEI-NE+MACCcity simulation exceeded these lifetimes by 1.2 days
24 (6.8 ± 1.0 d). The pronounced variability of the mean lifetime of BB BC was attributed to the
25 variability in regions and injection height. According to the injection scheme used (Sofiev et
26 al., 2013), continuous injection close to the PBL (around 65% of the mass of BC is emitted up
27 to 0.8 km, 90% up to 1.1 km) results in accumulation of BC in the troposphere, where longer
28 lifetime occurs compared to the PBL. This was likely the main reason for transport of BC into
29 the Arctic. For any soluble species emitted in the PBL, the lifetime is controlled by the
30 removal, which happens within a few days if it is not transported to the free troposphere. Two
31 weeks after being injected in the atmosphere, most of the tropospheric aerosol has been
32 scavenged through wet deposition, whereas aerosols that have been transported into the high
33 troposphere/lower stratosphere persist, given the absence of wet scavenging at these heights.



1 The total aerosol mass and the lifetimes are then dominated by the stratospheric loading
2 (Cassiani et al., 2013).

3 Mean aerosol lifetimes from global models are typically in the range of 3–7 days
4 (Benkovitz et al., 2004; Textor et al., 2006), very similar to our estimations for BC, but more
5 variable in this study due to the higher injection heights of BC in smoke plumes. As stated, in
6 the present case of wildfires in Northern Eurasia, the lifetimes and the behaviour of BC was
7 strongly affected by the fact that it was directly emitted aloft. Although 80–90% of BC was
8 emitted inside the PBL, nearly 65% of the BC was emitted near the PBL height, while 10%
9 was injected above (according to Sofiev et al., 2013).

10 In this study, we analyzed monthly values of both the Arctic BC burden and the mass
11 deposited in the Arctic for all BC sources (FEI-NE+MACCity) and for BC produced from BB
12 sources only over Northern Eurasia (FEI-NE). A strong seasonal variation can be seen in both
13 Arctic burden and deposition (Figure 4a, b, c and d). Relatively high BC burden from the
14 combined emissions of the FEI-NE+MACCity run occurred in winter (December–January,
15 Figure 4b), while two peaks were found in late spring and in summer for intense fire years.
16 The latest were clearly caused by spring and summer fire events over Northern Eurasia
17 (Figure 4). The higher winter values corresponded to the meridional transport of BC, mostly
18 emitted from anthropogenic sources (Figure 4a). These large increases in the burden were not
19 proportional among the different aerosol modes (hydrophilic and hydrophobic) and affected
20 mostly hydrophilic BC aerosol from vegetation fires. This indicated that wet scavenging was
21 less efficient than the rest of the year along the transport path between mid- and high-
22 latitudes. A spring maximum was also simulated for BC deposition over the Arctic. It was
23 caused by a combination of anthropogenic BC in the Northern Hemisphere and fires in
24 Northern Eurasia (Figure 4a and c), the majority of which occurred between March and May.
25 The annually deposited mass of BC over the Arctic exceeded the annual average for the
26 period 2002–2013 by 52% in 2003 and 86% in 2012.

27 There were three noteworthy findings. First, the year 2012 appeared to be a year when
28 BC transport to the Arctic was particularly efficient. Although the year itself (2012) was not
29 an extreme fire year (Figure S 1) in terms of fire detections, it appeared that the prevailing
30 winds and the lack of scavenging in mid-latitudes during June and July when fires were most
31 intense, favored transport and subsequent deposition to high-latitudes (120 kt from vegetation
32 fires only and 152 kt from all possible sources). Second, we simulated a higher relative
33 contribution of wet to total deposition in the Arctic (90%) than at mid-latitudes (69%). Third,



1 the annual mean lifetime of anthropogenic BC particles from BB was longer (6.8 d) than for
2 BC from combustion (5.6 d). These values are within the range of other published results
3 (e.g., 5.8 days from Park et al. (2005) and 7.3 days from Koch and Hansen (2005)).

4 **3.3 Geographic distribution of sources contributing to the Arctic BC**

5 In this section, we compare the contributions from different source regions and from
6 different emission types to the deposition of BC in the Arctic region. Several simulations with
7 BC tracers tagged by source region were carried out to isolate the different contributions. We
8 selected the following regions (Figure 5a): Europe, Asia, Siberia, Kazakhstan, and Mongolia,
9 as well as from the latitude bands 35°N to 40°N, 40°N to 50°N, 50°N to 60°N, above 60°N
10 (60°N–90°N), and also the entirety of Northern Eurasia. We discuss the results of these
11 separate simulations and compare them to our FEI-NE+MACCcity run (Figure 5). Each
12 simulation covered the whole period from 2002 to 2013.

13 Quinn et al. (2007) were the first to report that for BC over the Arctic, anthropogenic
14 sources dominated during winter and early spring Arctic Haze conditions. We estimated that
15 anthropogenic emissions accounted for 70% of the Arctic BC burden from all sources in the
16 North Hemisphere during winter and fall and for 40% during spring and summer when
17 vegetation fires are most frequent.

18 Vegetation fires from Northern Eurasia contributed 68% of the annual BC deposition
19 over the Arctic coming from that same region (Figure 5d), whereas anthropogenic emissions
20 constituted a lesser share (32%). Northern Eurasian vegetation fires were the most numerous
21 ones over the Northern Hemisphere; they contributed for 81% of the Arctic deposition of BC
22 from Northern Hemispheric fires (Figure 5d), while the rest came from other sources (e.g. BB in
23 North America).

24 Of the Northern Eurasian BB BC deposition in the Arctic, 95% was from Asia, while
25 only 5% came from Europe. On a more regional basis, Siberia contributed 46% of the
26 Northern Eurasian BB BC deposited in the Arctic, whereas Kazakhstan contributed 6%, and
27 Mongolia only 1%. The rest was shared between fire events in Europe (5%) and elsewhere in
28 Asia (42%) from areas that were not masked.

29 The relative contributions of fires at different latitudes to the Arctic BB BC deposition
30 were distributed as follows: fires from the 35°-40°N latitudinal band over Northern Eurasia
31 contributed only 7%, from 40°-50°N the contribution was 21%, 40% of this deposition came
32 from fires at 50°-60°N, and 32% from fires above 60°N (Figure 5c).



1 Moreover, we examined the vertical distribution of BC over the Arctic for the different
2 source regions (Figure 6). When emitted from Europe, BC over the Arctic was found mostly
3 below 5 km (either in the PBL or the low free troposphere), while BC emitted from Asia was
4 found in higher layers that extended up to the mid- to high- free troposphere (Figure 6).
5 Similar vertical distribution for aerosols have been reported by Stohl et al. (2002), who
6 estimated that aerosol originating from Asia was mixed throughout the entire troposphere
7 within a few days.

8 These findings can be discussed in light of the ones reported by other authors. For
9 instance, our results agree well with those of Hirdman et al. (2010a), who reported that the
10 Northern Eurasian region (Europe and Russia) was the main contributor to the Arctic surface
11 concentrations of BC and sulfate. The present study shows the importance of all the regions
12 north of 50°N. Stohl (2006) reported that Asia contributed 10 times less than Europe to the
13 Arctic BC surface concentrations, which was not supported by our findings for total BC. Our
14 results agreed with the conclusions of Koch and Hansen (2005), who reported that Europe
15 contributed 10% to the Arctic deposition of BC (anthropogenic and BB). In any case, all
16 surface measurements of BC over the Arctic indicated that the main contributors to the Arctic
17 BC during the summer were high-latitude sources (Hirdman et al., 2010a; Sharma et al.,
18 2013).

19 **4 Discussion**

20 **4.1 Observed and simulated BC concentrations at Arctic surface stations**

21 There are contradictory results in the literature about where geographically the Arctic
22 BC pollution originates. For example, Koch and Hansen (2005) estimated that Southeast Asia,
23 Europe and Russia contributed each about 20–25% of the Arctic pollution during January to
24 March period, whereas Stohl (2006) reported that Europe was the main contributor for the
25 Arctic BC concentration at the surface. In addition, Huang et al. (2010) stated that Russia
26 contributed 67% to the surface Arctic pollution, whereas Europe and North America were
27 18% and 15%, respectively (16-year observations from Alert). Northern Eurasia appeared to
28 be the main contributor in terms of Arctic BC during most seasons (Hirdman et al., 2010a).
29 More recently, Stohl et al. (2007) and Warneke et al. (2009) reported that boreal and
30 agricultural fires in Eastern Europe and in Siberia might be strong contributors to Arctic BC
31 especially in the spring. Furthermore, Stohl et al. (2013) highlighted gas-flaring emissions in
32 high latitudes as a major contributor to the Arctic BC.



1 Figure 8 compares the simulated surface BC concentrations from this study with in-situ
2 eBC and EC measurements from monitoring stations at Alert (Canada), Barrow (Alaska,
3 USA), Villum (Greenland, Denmark), Zeppelin (Ny-Ålesund, Svalbard, Norway), and Tiksi
4 (Russian Federation). The observations, when available, were represented for the entire period
5 of our simulations (2002–2013). At Zeppelin and Barrow stations, the measurements were
6 available between 2002 and 2013, at Alert from 2005 to 2013, at Villum for 2008 to 2011,
7 and at Tiksi station for 2009 to 2013. Figure 7 compares the simulated versus observed daily
8 surface concentrations by a Box and Whisker plot at the five Arctic stations (Alert, Barrow,
9 Villum, Tiksi, Zeppelin) for the period 2002 to 2013.

10 At Alert, there was a systematic underestimation in winter and early spring and an
11 overestimation in late spring and summer, when the station did not record any enhanced eBC
12 concentrations that would be attributed to vegetation fires in Northern Eurasia (Figure 8). At
13 Barrow, the model not only accurately estimated surface concentrations during winter, when
14 the Arctic Haze is important, but also in spring and summer, when vegetation fires persisted
15 (Figure 8). At Villum, the measured seasonality was reproduced quite well by the model and
16 also individual episodes of elevated BC surface concentrations in spring and summer were
17 captured and attributed to vegetation fires. At the Tiksi station, the comparison showed a
18 notable deviation from the measurements. Although some peaks in spring and summer were
19 captured, the model missed completely the high concentrations of eBC in winter and early
20 spring. Finally, at Zeppelin, it appeared that the anthropogenic BC contribution was slightly
21 underestimated (spring), while vegetation fires in Northern Eurasia elevated modeled surface
22 concentration of BC.

23 Looking at other inventories and results from the Lagrangian particle dispersion model
24 FLEXPART, we are convinced that local anthropogenic sources play an important role in the
25 apparition of these peaks (Eckhardt et al., 2015). It was already noted that our model
26 underestimated surface concentrations at Alert and Villum stations during the Arctic Haze
27 period. This is likely the consequence of an underestimation of Arctic transport in the model
28 or a misleading emission inventory used for anthropogenic sources (MACCity). To verify it,
29 we estimated surface concentrations of BC in the same longitude as the five Arctic stations,
30 but five and ten degrees south in latitude (Figure S 4). In all stations except Tiksi, surface
31 concentrations increased to the south confirming that the underestimation by our model over
32 the Arctic could be attributed to a too weak transport simulated towards the Arctic.

33 It has been reported that most models underestimated BC in the Arctic during winter
34 and early spring (Eckhardt et al., 2015), likely due to an improper representation of the



1 scavenging processes (lack of below-cloud scavenging for solid phase water), the different
2 emission profiles used for BC, and underestimated emission inventories used as input to the
3 models (e.g. Koch and Hansen, 2005; Liu et al, 2011; Jiao et al., 2014). Here, it is apparent
4 that the BC concentrations over the Arctic are reasonable with the current model version
5 compared to observations, with a tendency to underestimate winter concentrations and slightly
6 overestimate summer ones. The largest deviations occur at the station Tiksi, Russia. The
7 station is located only a few kilometers away from Tiksi town and local pollution is likely to
8 affect the measurements, as the town has both a small airport and a harbor. Despite these
9 drawbacks at Tiksi station, the data from the station has been used to estimate the sources in
10 Northern Eurasia (Cheng, 2014). Eckhardt et al. (2015) compared both surface- and aircraft
11 measurements of sulfate and BC in the Arctic to model output from eleven different models.
12 They found that the models generally underestimated the surface concentrations of BC and
13 sulfate in winter/spring, whereas concentrations in summer were overestimated. They also
14 found a strong correlation between surface measured sulfate and BC concentrations in
15 winter/spring (anthropogenic impact), which indicated that the sources contributing to sulfate
16 and BC were similar throughout the Arctic and that the aerosols were internally mixed and
17 undergo similar removal. Neither Eckhardt et al. (2015) nor Samset et al. (2013) could isolate
18 the reason to explain why some models performed better than the others.

19 In the present model configuration, we included emission inventory from FEI-NE and
20 MACCity's anthropogenic BC inside Northern Eurasia and MACCity (BB and
21 anthropogenic) outside Northern Eurasia (FEI-NE+MACCity), respectively, to evaluate if it
22 produced reliable results with respect to observations. The question that stemmed from this
23 comparison was whether or not existing datasets included all possible sources of BC
24 emission. This was examined by comparing FEI-NE+MACCity inventory with MACCity,
25 which included lower BC global emissions. Figure 8 depicts the difference of the average
26 atmospheric burden of BC between FEI-NE+MACCity and MACCity runs, while Figure S 5
27 and Figure S 6 show the same comparison for emissions and Arctic deposition of BC. It is
28 apparent that the difference in average atmospheric burden between FEI-NE+MACCity and
29 MACCity simulations (Figure 8) is positive over the Arctic showing that vegetation fires over
30 Northern Eurasia have a direct impact on the Arctic budget, especially during the most intense
31 fire years (2003, 2006, 2008, and 2012). The aforementioned impact extends up to North
32 America and may affect the BC concentrations there as well. Subsequently, the deviation of
33 the deposition of BC from Northern Eurasian vegetation fires relative to FEI-NE is shown to
34 be large over the Arctic (Figure S 6).



1 We also analyzed the influence of all anthropogenic and BB emissions from the regions
2 (defined in Table 1) to the average surface concentration of the Arctic stations (Figure 9). As
3 expected, the predominant contributor to the surface concentrations of the Arctic stations was
4 Northern Hemisphere anthropogenic emissions (29–55%) (e.g. Shaw et al., 2010). The
5 explanation is twofold. On one hand, transport of BC from the southern latitudes to the Arctic
6 takes place as the air-masses follow the trajectories of potential difference in temperature (a
7 dome effect), they are lifted up leaving the surface, especially from North America and Asia
8 (China). On the other hand, the transport from Russia/Siberia during the winter/spring is
9 closer to the surface due to large anthropogenic emissions that are also effectively transferred
10 from Europe. In addition, transport of BC from Russia/Siberia is less efficient during summer
11 due to pressure systems that block the BC transport. Fires from Northern Eurasia contributed
12 less BC to Barrow, Zeppelin, and Villum, while this pattern changed for Alert and Tiksi
13 stations (Figure 9). This shows that emissions from Northern Eurasia may extend up to the
14 American Arctic (Barrie, 1986). The region marked as “other” in Figure 9 stands for all BB
15 emissions occurring over the North Hemisphere, excluding Northern Eurasia, and shows that
16 4–42% of the surface concentrations may be due to fires in North America and other BB
17 sources. In all cases, fires in regions north of 50°N contributed the most, especially to Tiksi
18 station. Fires in the Asian part of Northern Eurasia contributed to the surface concentrations
19 of the stations by 13% to 57%, with the maximum at Tiksi station. This was expected since
20 this station is in the middle of the Northern Eurasian Arctic region and receives a lot of BC
21 emitted from BB in Siberia. The respective portion for fires occurring in Europe was
22 estimated to be 1–2% only. Similarly, BC emitted from Siberia contributed 9–43% to the
23 simulated surface concentrations at the stations (with a maximum in Tiksi station). We
24 estimated that the total of all vegetation fires in Northern Eurasia contributed around 56 ng m⁻³
25 ³, on average, to the Alert station (during spring and summer months), which is close to 89 ng
26 m⁻³ that Huang et al. (2010) estimated for USSR and European Union, although with different
27 geographic definitions than those assumed here, and also including anthropogenic emissions.
28 Gong et al. (2010) and Shindell et al. (2008) estimated that the Northern Eurasian
29 contribution to Alert varied between 80–90%, while our runs suggested that BB lower
30 contribution of 29%. Nevertheless, considering our comparison of modelling results with
31 surface observations for BC from the five Arctic stations, it should be noted that the
32 calculated contribution constituted an upper bound, especially when considering Asian and
33 Siberian regions.



1 4.2 Transport efficiency of BC to the Arctic

2 In this section, we examine the relative roles of different regions to emitting BC that
3 will ultimately be deposited over the Arctic. To do so, we computed the probability of BC
4 emitted from different regions to reach the Arctic. We defined the transport efficiency to the
5 Arctic as the ratio between the mass of BC deposited in the Arctic to the total mass of BC
6 emitted from a given region. These estimates were obtained by masking the same
7 geographical regions as in section 3.3 (anthropogenic sources in the Northern Hemisphere,
8 vegetation fires in Europe, Asia, between 35°N–40°N, 40°N–50°N, 50°N–60°N and above
9 60°N) and simulating fires that occurred inside the masked areas for the period 2012–2013
10 (Table 1).

11 Figure 10 depicts the transport efficiency with which BC from vegetation fires reached
12 the Arctic for the different geographic regions. The results clearly show that anthropogenic
13 BC from large emitting regions in southeastern Asia and other Asian regions were not
14 transported efficiently to the Arctic. The main source contributing to Arctic deposition was
15 BB in Northern Eurasia with a transport efficiency of 10–32% during spring and summer, and
16 1–6% in autumn and winter. Overall, the transport and subsequent deposition of BC from
17 Asia was more effective than from Europe (12% of the BB emissions from Asia were
18 deposited in the Arctic, whereas only 5% of the European BB emissions reach the Arctic),
19 which was attributed to the fact that European BC tends to remain close to the PBL (Figure
20 10), whereas the Asian BC mixes up rapidly into the free troposphere (Stohl et al., 2002).
21 Therefore, European BC was much more affected by removal processes since its transport to
22 the Arctic is much less efficient.

23 In contrast, Siberian BC was deposited very efficiently to the Arctic in summer and
24 autumn similar to fires above 60°N (besides, Siberia covers the Asian part of the 60°N–90°N
25 area). However, it was evident from our results, that in our model the most efficient regional
26 transport of BC to the Arctic occurred in the summer months and was attributed to vegetation
27 fires in Kazakhstan and Mongolia (apart from Siberia, Figure 10). To summarize these
28 results, the highest transport efficiencies in our model occurred in the spring and summer for
29 all Northern Eurasia. This may be a result of (i) extreme fire events, (ii) the relatively weak
30 removal processes occurring in mid- and high-latitudes which favor transport without removal
31 of BC, and (iii) the imposed fixed injection profiles used in these simulations.



1 5 Conclusions

2 The present study focused on the impact of vegetation fires occurring in Northern
3 Eurasia on BC deposition in the Arctic. For this reason, a three dimensional global transport
4 model (LMDz-OR-INCA) was used to simulate fire events that took place during 2002–2013.
5 Anthropogenic emissions were adopted from MACCity inventory, while BB emissions within
6 Northern Eurasia were from FEI-NE and beyond Northern Eurasia from MACCity's GFEDv3
7 database.

8 A total of 3.0×10^6 km² was burned during the 12-year period in Northern Eurasia with
9 the majority to be grassland and forest fires. Total global emissions of BC ranged from 8.02
10 Tg to 9.48 Tg (average: 8.42 ± 0.43 Tg yr⁻¹) with the highest ones recorded for the years 2003,
11 2006, 2008, and 2012. The annual emissions from vegetation fires in Northern Eurasia were
12 estimated to be between 0.45 and 2.19 Tg (average: 0.86 ± 0.51 Tg yr⁻¹). Comparing to the
13 MACCity emission inventory, our simulations suggested that 10–17% (average: 8%) more
14 BC was emitted by FEI-NE+MACCity, while FEI-NE biomass burning emissions were 3.5
15 times higher than GFED3.

16 The annual mean deposition of BC in the Arctic from vegetation fires in Northern
17 Eurasia was found to be 65 ± 28 kt yr⁻¹ for the 12-year period, which represents 45–78% of the
18 BC deposited from all possible sources and origins. The combined run (FEI-NE+MACCity)
19 brought around 55% (1218 versus 675 kt in total for the 12-year period) more BC to deposit
20 over the Arctic environment comparing to the conventional MACCity emission inventory.

21 Arctic burden showed a strong seasonal variation, which peaks during late winter and
22 early spring in the presence of the Arctic Haze. The peak in winter depicted the latitudinal
23 transport of BC mainly from anthropogenic sources in Europe, whereas the peak in spring and
24 summer clearly stemmed from the fire episodes in Northern Eurasia. The annual mass of BC
25 deposited over the Arctic increased during the most intense fire years (37% in 2009 to 181%
26 in 2012) in comparison to the annual average for the period of 2002–2013.

27 Fires occurring in the Northern Hemisphere contributed 68% to the simulated
28 deposition of BC in the Arctic, while the rest originated from anthropogenic sources. The
29 majority of the vegetation fires in the Northern Hemisphere was attributed to Northern
30 Eurasian vegetation fires (85%), of which Asia contributed 81% and Europe only 4%. These
31 results were consistent with what other researchers have reported, as Asian BC experienced
32 fast elevation to the free troposphere and hence long-range transport.

33 The present results were compared to surface observations from five stations (Alert,
34 Barrow, Villum, Tiksi, and Zeppelin) showing relatively good results and in most stations



1 capturing the trend in surface BC concentrations (a notable deviation was observed at Alert
2 Alert). We estimated that vegetation fires in Northern Eurasia contributed 14% to 57% to the
3 surface environment of these stations, mostly affected by fires that took place in Siberia. This
4 showed the importance of fires occurring over Northern Eurasia in the Arctic BC budget.
5 However, anthropogenic sources also remain essential contributing 29% to 54% to the surface
6 of the Arctic stations.

7

8 **Acknowledgements**

9 This study was supported by the US Forest Service, Rocky Mountain Research Station. It was
10 also granted access to the HPC resources of [CCRT/TGCC/CINES/IDRIS] under the
11 allocation 2012-t2012012201 made by GENCI (Grand Equipement National de Calcul
12 Intensif). We would also like to acknowledge the World Data Centre for Aerosol, in which
13 BC measurements from Arctic stations are hosted (<http://ebas.nilu.no>). Authors would like to
14 acknowledge Dan Veber for calibration and instrument maintenance, other technicians,
15 students and staff of CFS Alert for maintaining the site.

16



1 **References**

- 2 Ackerman, A. S., Toon, O. B., Stevens, D. E., Heymsfield, A. J., Ramanathan, V., and
3 Welton, E. J.: Reduction of tropical cloudiness by soot, *Science*, 288, 1042–1047, 2000.
- 4 Barrie, L. A.: Arctic air pollution: An overview of current knowledge, *Atmos. Environ.*, 20
5 (4), 643–663, 1983.
- 6 Benkovitz, C. M., Schwartz, S. E., Jensen, M. P., Miller, M. A., Easter, R. C., and Bates, T.
7 S.: Modeling atmospheric sulfur over the Northern Hemisphere during the Aerosol
8 Characterization Experiment 2 experimental period, *J. Geophys. Res.*, 109, D22207,
9 2004.
- 10 Bond, T. C., and Bergstrom, R. W.: Light absorption by carbonaceous particles: an
11 investigative review, *Aerosol Sci. Tech.*, 40, 27–67, doi:10.1080/02786820500421521,
12 2006.
- 13 Bond, T. C., Doherty, S. J., Fahey, D. W., Forster, P. M., Berntsen, T., DeAngelo, B. J.,
14 Flanner, M. G., Ghan, S., Kärcher, B., Koch, D., Kinne, S., Kondo, Y., Quinn, P. K.,
15 Sarofim, M. C., Schultz, M. G., Schulz, M., Venkataraman, C., Zhang, H., Zhang, S.,
16 Bellouin, N., Guttikunda, S. K., Hopke, P. K., Jacobson, M. Z., Kaiser, J. W., Klimont,
17 Z., Lohmann, U., Schwarz, J. P., Shindell, D., Storelvmo, T., Warren, S. G., and Zender
18 C. S.: Bounding the role of black carbon in the climate system: A scientific assessment,
19 *J. Geophys. Res. Atmos.*, 118, 5380–5552, 2013.
- 20 Browse, J., Carslaw, K. S., Arnold, S. R., Pringle, K., and Boucher, O.: The scavenging
21 processes controlling the seasonal cycle in Arctic sulphate and black carbon aerosol,
22 *Atmos. Chem. Phys.*, 12, 6775–6798, doi:10.5194/acp-12-6775-2012, 2012.
- 23 Bond, T. C., Doherty, S. J., Fahey, D. W., Forster, P. M., Berntsen, T., DeAngelo, B. J.,
24 Flanner, M. G., Ghan, S., Kärcher, B., Koch, D., Kinne, S., Kondo, Y., Quinn, P. K.,
25 Sarofim, M. C., Schultz, M. G., Schulz, M., Venkataraman, C., Zhang, H., Zhang, S.,
26 Bellouin, N., Guttikunda, S. K., Hopke, P. K., Jacobson, M. Z., Kaiser, J. W., Klimont,
27 Z., Lohmann, U., Schwarz, J. P., Shindell, D., Storelvmo, T., Warren, S. G., and
28 Zender, C. S.: Bounding the role of black carbon in the climate system: A scientific
29 assessment, *J. Geophys. Res.*, 118, 5380–5552, doi:10.1002/jgrd.50171, 2013.
- 30 Cassiani, M., Stohl, A., and Eckhardt, S.: The dispersion characteristics of air pollution from
31 the world's megacities, *Atmos. Chem. Phys.*, 13, 9975–9996, 2013.
- 32 Cavalli, F., Viana, M., Yttri, K. E., Genberg, J., and Putaud, J. P.: Toward a standardised
33 thermal- optical protocol for measuring atmospheric organic and elemental carbon: the
34 EUSAAR protocol, *Atmos. Meas. Tech.*, 3, 79–89, doi:10.5194/amt-3-79-2010, 2010.



- 1 Cheng M.-D.: Geolocating Russian sources for Arctic black carbon, *Atmos. Environ.*, **92**,
- 2 398–410, 2014.
- 3 Chung, S. H. and Seinfeld, J. H.: Global distribution and climate forcing of carbonaceous
- 4 aerosols, *J. Geophys. Res.*, **107** (D19), 4407, 2002.
- 5 Clarke, A. D., and Noone, K. J.: Soot in the Arctic snowpack: A cause for perturbations in
- 6 radiative transfer, *Atmos. Environ.*, **19**(12), 2045–2053, 1985.
- 7 Croft, B., Pierce, J. R., and Martin, R. V.: Interpreting aerosol lifetimes using the GEOS-
- 8 Chem model and constraints from radionuclide measurements, *Atmos. Chem. Phys.*
- 9 *Discuss.*, **13**, 32391–32421, 2013.
- 10 ECMWF: ERA Interim, Daily fields, available at:
- 11 http://apps.ecmwf.int/datasets/data/interim_full_daily/, 2014.
- 12 Eckhardt, S., Hermansen, O., Grythe, H., Fiebig, M., Stebel, K., Cassiani, M., Baecklund, A.,
- 13 and Stohl, A.: The influence of cruise ship emissions on air pollution in Svalbard – a
- 14 harbinger of a more polluted Arctic?, *Atmos. Chem. Phys.*, **15**, 9413–9433, 2015.
- 15 Eckhardt, S., Quennehen, B., Olivié, D. J. L., Berntsen, T. K., Cherian, R., Christensen, J. H.,
- 16 Collins, W., Crepinsek, S., Daskalakis, N., Flanner, M., Herber, A., Heyes, C.,
- 17 Hodnebrog, Ø., Huang, L., Kanakidou, M., Klimont, Z., Langner, J., Law, K. S.,
- 18 Massling, A., Myriokefalitakis, S., Nielsen, I. E., Nøjgaard, J. K., Quaas, J., Quinn, P.
- 19 K., Raut, J.-C., Rumbold, S. T., Schulz, M., Skeie, R. B., Skov, H., Lund, M. T., Uttal,
- 20 T., von Salzen, K., Mahmood, R., and Stohl, A.: Current model capabilities for
- 21 simulating black carbon and sulfate concentrations in the Arctic atmosphere: a multi-
- 22 model evaluation using a comprehensive measurement data set, *Atmos. Chem. Phys.*,
- 23 **15**, 9413–9433, 2015.
- 24 Eleftheriadis, K., Vratolis S., and Nyeki S.: Aerosol black carbon in the European Arctic:
- 25 Measurements at Zeppelin station, Ny-Ålesund, Svalbard from 1998–2007, *Geophys.*
- 26 *Res. Lett.*, **36**, L02809, 2009.
- 27 Elvidge Ch. D., Ziskin, D., Baugh, K. E., Tuttle, B. T., Ghosh, T., Pack, D.W., Erwin, E. H.,
- 28 and Zhizhin, M.: A fifteen year record of global natural gas flaring derived from
- 29 satellite data, *Energies*, **2**, 595–622, doi:10.3390/en20300595, 2009.
- 30 Emanuel, K. A.: A scheme for representing cumulus convection in large-scale models, *J.*
- 31 *Atmos. Sci.*, **48**, 2313–2335, 1991.
- 32 Evangelioiu, N., Balkanski, Y., Cozic, A., and Møller, A.P.: Simulations of the transport and
- 33 deposition of ¹³⁷Cs over Europe after the Chernobyl NPP accident: influence of varying



- 1 emission-altitude and model horizontal and vertical resolution, Atmos. Chem. Phys. 13,
2 7183–7198, 2013.
- 3 Flanner, M. G., Zender C. S., Randerson J. T., and Rasch P. J.: Present - day climate forcing
4 and response from black carbon in snow, J. Geophys. Res., 112, D11202, 2007.
- 5 Flanner, M. G., Zender C. S., Hess P. G., Mahowald N. M., Painter T. H., Ramanathan V.,
6 and Rasch P. J.: Springtime warming and reduced snow cover from carbonaceous
7 particles, Atmos. Chem. Phys., 9(7), 2481–2497, 2009.
- 8 Forster, C., Wandering, U., Wotawa, G., James, P., Mattis, I., Althausen, D., Simmonds, P.,
9 O'Doherty, S., Jennings, S. G., Kleefeld, C., Schneider, J., Trickl, T., Kreipl, S., Jäger,
10 H., and Stohl A.: Transport of boreal forest fire emissions from Canada to Europe, J.
11 Geophys. Res., 106(D19), 22887–22906, 2001.
- 12 Friedl, M. A., McIver, D. K., Hodges, J. C. F., Zhang, X. Y., Muchoney, D., Strahler, A. H.,
13 Woodcock, C. E., Gopal, S., Schneider, A., Cooper, A., Baccini, A., Gao, F., and
14 Schaaf, C.: Global land cover mapping from MODIS: Algorithms and early results,
15 Remote Sens. Environ., 83, 287–302, 2002.
- 16 Fromm, M., Bevilacqua, R., Servranckx, R., Rosen, J., Thayer, J.P., Herman, J., and Larko
17 D.: Pyro-cumulonimbus injection of smoke to the stratosphere: Observations and
18 impact of a super blowup in northwestern Canada on 3–4 August 1998, J. Geophysical
19 Research, 110, D08205, 2005.
- 20 Garrett, T. J., and Zhao C.: Increased Arctic cloud longwave emissivity associated with
21 pollution from mid - latitudes, Nature, 440(7085), 787–789, 2006.
- 22 GFMC: Reports on fire smoke pollution in Europe generated by wildland fires in the Russian
23 Federation, available at: [http://www.fire.uni-](http://www.fire.uni-freiburg.de/media/2006/05/news_20060518_uk.htm)
24 [freiburg.de/media/2006/05/news_20060518_uk.htm](http://www.fire.uni-freiburg.de/media/2006/05/news_20060518_uk.htm); [http://www.fire.uni-](http://www.fire.uni-freiburg.de/media/2006/08/news_20060825_fin.htm)
25 [freiburg.de/media/2006/08/news_20060825_fin.htm](http://www.fire.uni-freiburg.de/media/2006/08/news_20060825_fin.htm); [http://www.fire.uni-](http://www.fire.uni-freiburg.de/media/2006/06/news_20060608_fi.htm)
26 [freiburg.de/media/2006/06/news_20060608_fi.htm](http://www.fire.uni-freiburg.de/media/2006/06/news_20060608_fi.htm); [http://www.fire.uni-](http://www.fire.uni-freiburg.de/media/2006/06/news_20060608_fi4.htm)
27 [freiburg.de/media/2006/06/news_20060608_fi4.htm](http://www.fire.uni-freiburg.de/media/2006/06/news_20060608_fi4.htm); [http://www.fire.uni-](http://www.fire.uni-freiburg.de/media/2006/06/news_20060608_fi3.htm)
28 [freiburg.de/media/2006/06/news_20060608_fi3.htm](http://www.fire.uni-freiburg.de/media/2006/06/news_20060608_fi3.htm); [http://www.fire.uni-](http://www.fire.uni-freiburg.de/media/2006/06/news_20060608_fi2.htm)
29 [freiburg.de/media/2006/06/news_20060608_fi2.htm](http://www.fire.uni-freiburg.de/media/2006/06/news_20060608_fi2.htm); [http://www.fire.uni-](http://www.fire.uni-freiburg.de/GFMCnew/2006/05/0501/20060501_ru.htm)
30 [freiburg.de/GFMCnew/2006/05/0501/20060501_ru.htm](http://www.fire.uni-freiburg.de/GFMCnew/2006/05/0501/20060501_ru.htm), 2006.
- 31 Gong, S. L., Zhao, T. L., Sharma, S., Toom-Sauntry, D., Lavoue, D., Zhang, X. B.,
32 Leaitch, W. R., and Barrie, L.: Identification of trends and inter-annual variability of



- 1 sulphate and black carbon in the Canadian High Arctic: 1981 to 2007, *J. Geophys. Res.-*
2 *Atmos.*, 115, D07305, 2010.
- 3 Granier, C., Bessagnet, B., Bond, T., D'Angiola, A., van der Gon, H. D., Frost, G. J., Heil, A.,
4 Kaiser, J. W., Kinne, S., Klimont, Z., Kloster, S., Lamarque, J.-F., Liousse, C., Masui,
5 T., Meleux, F., Mieville, A., Ohara, T., Raut, J. C., Riahi, K., Schultz, M. G., Smith, S.
6 J., Thompson, A., van Aardenne, J., van der Werf, G. R., and van Vuuren, D. P.:
7 Evolution of anthropogenic and biomass burning emissions of air pollutants at global
8 and regional scales during the 1980-2010 period, *Climatic Change*, 109, 163-190, 2001.
- 9 Hansen, J., and Nazarenko L.: Soot climate forcing via snow and ice albedos, *Proc. Natl.*
10 *Acad. Sci. U. S. A.*, 101(2), 423–428, 2004.
- 11 Hao, W. M., Bondarenko, O. O., Zibtsev, S., and Hutton, D.: Vegetation fires, smoke
12 emissions, and dispersion of radionuclides in the Chernobyl exclusion zone, in
13 *Wildland Fires and Air Pollution*, *Dev. Environ. Sci.*, vol. 8, edited by A. Bytnerowicz
14 et al., chap. 12, pp. 265–276, 2009, Elsevier, Amsterdam.
- 15 Hao, W. M., Petkov, A., Nordgren, B. L., Silverstein, R. P., Corley, R., Urbanski, S. P.,
16 Evangeliou, N., Balkanski, Y., and Kinder, B.: Daily black carbon emissions from fires
17 in Northern Eurasia from 2002 to 2013, *Atmos. Chem. Phys. Discuss.*, this issue.
- 18 Hauglustaine, D. A., Hourdin, F., Walters, S., Jourdain, L., Filiberti, M.-A., Lamarque, J.-F.,
19 and Holland, E. A.: Interactive chemistry in the Laboratoire de Météorologie
20 Dynamique general circulation model: description and background tropospheric
21 chemistry evaluation, *J. Geophys. Res.*, 109, D04314, 2004.
- 22 Hirdman, D., Sodemann, H., Eckhardt, S., Burkhardt, J. F., Jefferson, A., Mefford, T., Quinn,
23 P. K., Sharma, S., Ström, J., and Stohl A.: Source identification of short - lived air
24 pollutants in the Arctic using statistical analysis of measurement data and particle
25 dispersion model output, *Atmos. Chem. Phys.*, 10, 669–693, 2010a.
- 26 Hirdman, D., J. F. Burkhardt, H. Sodemann, S. Eckhardt, A. Jefferson, P. K. Quinn, S. Sharma,
27 J. Ström, and Stohl A.: Long-term trends of black carbon and sulphate aerosol in the
28 Arctic: changes in atmospheric transport and source region emissions, *Atmos. Chem.*
29 *Phys.*, 10, 9351–9368, 2010b.
- 30 Hourdin F., and Issartel J. P.: Sub-surface nuclear tests monitoring through the CTBT xenon
31 network, *Geophys. Res. Lett.*, 27, 2245–2248, 2000.
- 32 Hourdin, F., and Armengaud, A.: The use of finite-volume methods for atmospheric
33 advection of trace species – 1. test of various formulations in a general circulation
34 model, *Mon. Weather Rev.*, 127, 822–837, 1999.



- 1 Hourdin, F., Musat, I., Bony, S., Braconnot, P., Codron, F., Dufresne, J.-L., Fairhead, L.,
2 Filiberti, M.-A., Friedlingstein, P., Grandpeix, J.-Y., Krinner, G., Levan, P., Li, Z.-X.,
3 and Lott, F.: The LMDZ4 general circulation model: climate performance and
4 sensitivity to parametrized physics with emphasis on tropical convection, *Clim.*
5 *Dynam.*, 27, 787–813, 2006.
- 6 Huang, L., Gong, S. L., Sharma, S., Lavoué, D., and Jia, C. Q.: A trajectory analysis of
7 atmospheric transport of black carbon aerosols to Canadian high Arctic in winter and
8 spring (1990–2005), *Atmos. Chem. Phys.*, 10, 5065–5073, 2010.
- 9 IFFN: Recent Trends of Forest Fires in Central Asia and Opportunities for Regional
10 Cooperation in Forest Fire Management, available at: [http://www.fire.uni-
12 freiburg.de/iffn/iffn_31/16b-IFFN-31-Central-Asia-2.pdf](http://www.fire.uni-
11 freiburg.de/iffn/iffn_31/16b-IFFN-31-Central-Asia-2.pdf), 2004.
- 12 Jiao, C., Flanner, M. G., Balkanski, Y., Bauer, S. E., Bellouin, N., Berntsen, T. K., Bian, H.,
13 Carslaw, K. S., Chin, M., De Luca, N., Diehl, T., Ghan, S. J., Iversen, T., Kirkevåg, A.,
14 Koch, D., Liu, X., Mann, G. W., Penner, J. E., Pitari, G., Schulz, M., Seland, Ø., Skeie,
15 R. B., Steenrod, S. D., Stier, P., Takemura, T., Tsigaridis, K., van Noije, T., Yun, Y.,
16 and Zhang, K.: An AeroCom assessment of black carbon in Arctic snow and sea ice,
17 *Atmos. Chem. Phys.*, 14, 2399–2417, 2014.
- 18 Jost, H.-J., Drdla, K., Stohl, A., Pfister, L., Loewenstein, M., Lopez, J. P., Hudson, P. K.,
19 Murphy, D. M., Cziczko, D. J., Fromm, M., Bui, T. P., Dean-Day, J., Gerbig, C.,
20 Mahoney, M. J., Richard, E. C., Spichtinger, N., Pittman, J. V., Weinstock, E. M.,
21 Wilson, J. C., and Xueref, I.: In-situ observations of mid-latitude forest fire plumes deep
22 in the stratosphere, *Geophys. Res. Lett.* 31, L11101, doi:10.1029/2003GL019253, 2004.
- 23 Klonecki, A., Hess, P., Emmons, L., Smith, L., Orlando, J., and Blake, D.: Seasonal changes
24 in the transport of pollutants into the Arctic troposphere – model study, *J. Geophys.*
25 *Res.*, 108 (D4), 8367, 2003.
- 26 Koch, D., and Hansen, J.: Distant origins of Arctic black carbon: A Goddard Institute for
27 Space Studies ModelE experiment, *J. Geophys. Res.*, 110, D04204, 2005.
- 28 Krinner, G., Viovy, N., de Noblet-Ducoudre, N., Ogee, J., Polcher, J., Friedlingstein, P.,
29 Ciais, P., Sitch, S., and Prentice, I. C.: A dynamic global vegetation model for studies of
30 the coupled atmosphere-biosphere system, *Global Biogeochem. Cy.*, 19, GB1015, 2005.
- 31 Lamarque, J.-F., Bond, T. C., Eyring, V., Granier, C., Heil, A., Klimont, Z., Lee, D., Liousse,
32 C., Mieville, A., Owen, B., Schultz, M. G., Shindell, D., Smith, S. J., Stehfest, E., Van
33 Aardenne, J., Cooper, O. R., Kainuma, M., Mahowald, N., McConnell, J. R., Naik, V.,
34 Riahi, K., and van Vuuren, D. P.: Historical (1850–2000) gridded anthropogenic and



- 1 biomass burning emissions of reactive gases and aerosols: methodology and
2 application, *Atmos. Chem. Phys.*, 10, 7017–7039, 2010.
- 3 Law, K. S., and Stohl, A.: Arctic air pollution: Origins and impacts, *Science*, 315(5818),
4 1537–1540, 2007.
- 5 Lee, Y. H., Lamarque, J.-F., Flanner, M. G., Jiao, C., Shindell, D. T., Berntsen, T., Bisiaux,
6 M. M., Cao, J., Collins, W. J., Curran, M., Edwards, R., Faluvegi, G., Ghan, S.,
7 Horowitz, L. W., Mc-Connell, J. R., Myhre, G., Nagashima, T., Naik, V., Rumbold, S.
8 T., Skeie, R. B., Sudo, K., Takemura, T., and Thevenon, F.: Evaluation of preindustrial
9 to present-day black carbon and its albedo forcing from Atmospheric Chemistry and
10 Climate Model Intercomparison Project (ACCMIP), *Atmos. Chem. Phys.*, 13, 2607–
11 2634, 2013.
- 12 Lee, Y. H., Lamarque, J.-F., Flanner, M. G., Jiao, C., Shindell, D. T., Berntsen, T., Bisiaux,
13 M. M., Cao, J., Collins, W. J., Curran, M., Edwards, R., Faluvegi, G., Ghan, S.,
14 Horowitz, L. W., Mc-Connell, J. R., Myhre, G., Nagashima, T., Naik, V., Rumbold, S.
15 T., Skeie, R. B., Sudo, K., Takemura, T., and Thevenon, F.: Corrigendum to
16 “Evaluation of preindustrial to present-day black carbon and its albedo forcing from
17 Atmospheric Chemistry and Climate Model Intercomparison Project (ACCMIP)”
18 published in *Atmos. Chem. Phys.*, 13, 2607–2634, 2013, *Atmos. Chem. Phys.*, 13,
19 6553–6554, 2013.
- 20 Liu, J., Fan, S., Horowitz, L. W., Levy, H.: Evaluation of factors controlling long – range
21 transport of black carbon to the Arctic, *J. Geophys. Res.*, 116, D04307, 2011.
- 22 Lubin, D., and Vogelmann, A. M.: A climatologically significant aerosol long wave indirect
23 effect in the Arctic, *Nature*, 439(7075), 453–456, 2006.
- 24 Myhre, G., Samset, B. H., Schulz, M., Balkanski, Y., Bauer, S., Berntsen, T. K., Bian, H.,
25 Bellouin, N., Chin, M., Diehl, T., Easter, R. C., Feichter, J., Ghan, S. J.,
26 Hauglustaine, D., Iversen, T., Kinne, S., Kirkevåg, A., Lamarque, J.-F., Lin, G., Liu, X.,
27 Lund, M. T., Luo, G., Ma, X., van Noije, T., Penner, J. E., Rasch, P. J., Ruiz, A.,
28 Seland, Ø., Skeie, R. B., Stier, P., Takemura, T., Tsigaridis, K., Wang, P., Wang, Z.,
29 Xu, L., Yu, H., Yu, F., Yoon, J.-H., Zhang, K., Zhang, H., and Zhou, C.: Radiative
30 forcing of the direct aerosol effect from AeroCom Phase II simulations, *Atmos. Chem.*
31 *Phys.*, 13, 1853–1877, 2013.
- 32 Nedelec, P., V. Thouret, J. Brioude, B. Sauvage, J.-P. Cammas, and A. Stohl (2005): Extreme
33 CO concentrations in the upper troposphere over North-East Asia in June 2003 from the



- 1 in-situ MOZAIC aircraft data, *Geophys. Res. Lett.* 32, L14807,
2 doi:10.1029/2005GL023141.
- 3 Park, R. J., Jacob, D. J., Palmer, P. I., Clarke, A. D., Weber, R. J., Zondlo, M. A., Eisele, F.
4 L., Bandy, A. R., Thornton, D. C., Sachse, G. W., and Bond, T. C.: Export efficiency of
5 black carbon aerosol in continental outflow: Global implications, *J. Geophys. Res.*, 110,
6 D11205, doi:10.1029/2004JD005432, 2005.
- 7 Petzold, A., Ogren, J. A., Fiebig, M., Laj, P., Li, S.-M., Baltensperger, U., Holzer-Popp, T.,
8 Kinne, S., Pappalardo, G., Sugimoto, N., Wehrli, C., Wiedensohler, A., and Zhang, X.-
9 Y.: Recommendations for reporting "black carbon" measurements, *Atmos. Chem.*
10 *Phys.*, 13, 8365–8379, 2013.
- 11 Quinn, P. K., Shaw, G., Andrews, E., Dutton, E. G., Ruoho-Airola, T., and Gong, S. L.:
12 Arctic haze: current trends and knowledge gaps, *Tellus B*, 59, 99–114, 2007.
- 13 Quinn, P. K., Jacob, D. J., Palmer, P. I., Clarke, A. D., Weber, R. J., Zondlo, M. A., Eisele, F.
14 L., Bandy, A. R., Thornton, D. C., Sachse, G. W., and Bond, T. C.: Short - lived
15 pollutants in the Arctic: Their climate impact and possible mitigation strategies, *Atmos.*
16 *Chem. Phys.*, 8(6), 1723–1735, 2008.
- 17 Samset, B. H., Myhre, G., Herber, A., Kondo, Y., Li, S.-M., Moteki, N., Koike, M., Oshima,
18 N., Schwarz, J. P., Balkanski, Y., Bauer, S. E., Bellouin, N., Berntsen, T. K., Bian, H.,
19 Chin, M., Diehl, T., Easter, R. C., Ghan, S. J., Iversen, T., Kirkevåg, A., Lamarque, J.-
20 F., Lin, G., Liu, X., Penner, J. E., Schulz, M., Seland, Ø., Skeie, R. B., Stier, P.,
21 Takemura, T., Tsigaridis, K., and Zhang, K.: Modelled black carbon radiative forcing
22 and atmospheric lifetime in AeroCom Phase II constrained by aircraft observations,
23 *Atmos. Chem. Phys.*, 14, 12465–12477, 2014.
- 24 Schulz, M., Balkanski, Y., Dulac, F., and Guelle, W.: Role of aerosol size distribution and
25 source location in a three-dimensional simulation of a Saharan dust episode tested
26 against satellite derived optical thickness, *J. Geophys. Res.*, 103, 10579–10592, 1998.
- 27 Schulz, M.: Constraining Model Estimates of the Aerosol Radiative Forcing, Thèse
28 d'Habilitation à Diriger des Recherches, Université Pierre et Marie Curie, Paris VI,
29 2007.
- 30 Sharma, S., Andrews, E., Barrie, L. A., Ogren, J. A., and Lavoué D.: Variations and sources
31 of the equivalent black carbon in the high Arctic revealed by long-term observations at
32 Alert and Barrow: 1989–2003, *J. Geophys. Res.*, 111, D14208, 2006.



- 1 Sharma, S., Ishizawa, M., Chan, D., Lavoue, D., Andrews, E., Eleftheriadis, K., and
2 Maksyutov, S.: 16 year simulation of Arctic black carbon: transport, source
3 contribution, and sensitivity analysis on deposition, *J. Geophys. Res.-Atmos.*, 118, 943–
4 964, doi:10.1029/2012jd017774, 2013.
- 5 Shaw, G. E.: The Arctic haze phenomenon, *Bull. Am. Meteorol. Soc.*, 76(12), 2403–2413,
6 1995.
- 7 Shaw, P. M., Russell, L. M., Jefferson, A., and Quinn, P. K.: Arctic organic aerosol
8 measurements show particles from mixed combustion in spring haze and from frost
9 flowers in winter, *Geophys. Res. Lett.*, 37, L10803, doi:10.1029/2010GL042831, 2010.
- 10 Shindell, D. T., Chin, M., Dentener, F., Doherty, R. M., Faluvegi, G., Fiore, A. M., Hess, P.,
11 Koch, D. M., MacKenzie, I. A., Sanderson, M. G., Schultz, M. G., Schulz, M.,
12 Stevenson, D. S., Teich, H., Textor, C., Wild, O., Bergmann, D. J., Bey, I., Bian, H.,
13 Cuvelier, C., Duncan, B. N., Folberth, G., Horowitz, L. W., Jonson, J., Kaminski, J. W.,
14 Marmer, E., Park, R., Pringle, K. J., Schroeder, S., Szopa, S., Takemura, T., Zeng, G.,
15 Keating, T. J., and Zuber, A.: A multi-model assessment of pollution transport to the
16 Arctic, *Atmos. Chem. Phys.*, 8, 5353–5372, 2008.
- 17 Sirois, A., and Barrie, L. A.: Arctic lower tropospheric aerosol trends and composition at
18 Alert, Canada: 1980–1995, *J. Geophys. Res.*, 104(D9), 11599–11618, 1999.
- 19 Sofiev, M., Vankevich, R., Ermakova, T., and Hakkarainen, J.: Global mapping of maximum
20 emission heights and resulting vertical profiles of wildfire emissions, *Atmos. Chem.*
21 *Phys.*, 13, 7039–7052, 2013.
- 22 Spackman, J. R., Gao, R. S., Neff, W. D., Schwarz, J. P., Watts, L. A., Fahey, D. W.,
23 Holloway, J. S., Ryerson, T. B., Peischl, J., and Brock, C. A.: Aircraft observations of
24 enhancement and depletion of black carbon mass in the springtime Arctic, *Atmos.*
25 *Chem. Phys.*, 10, 9667–9680, 2010.
- 26 Stohl, A., Berg, T., Burkhart, J. F., Fjårraa, A. M., Forster, C., Herber, A., Hov, Ø., Lunder,
27 C., McMillan, W. W., Oltmans, S., Shiobara, M., Simpson, D., Solberg, S., Stebel, K.,
28 Ström, J., Tørseth, K., Treffeisen, R., Virkkunen, K., and Yttri, K. E.: Arctic smoke –
29 record high air pollution levels in the European Arctic due to agricultural fires in
30 Eastern Europe in spring 2006, *Atmos. Chem. Phys.*, 7, 511–534, doi:10.5194/acp-7-
31 511-2007, 2007.
- 32 Stohl, A., Klimont, Z., Eckhardt, S., Kupiainen, K., Shevchenko, V. P., Kopeikin, V. M., and
33 Novigatsky, A. N.: Black carbon in the Arctic: the underestimated role of gas flaring
34 and residential combustion emissions, *Atmos. Chem. Phys.*, 13, 8833–8855, 2013.



- 1 Stohl, A.: Characteristics of atmospheric transport into the Arctic troposphere, *J. Geophys.*
2 *Res.*, 111, D11306, 2006.
- 3 Stohl, A., Eckhardt, S., Forster, C., James, P., and Spichtinger, N.: On the pathways and
4 timescales of intercontinental air pollution transport, *J. Geophys. Res.*, 107(D23), 4684,
5 2002.
- 6 Textor, C., Schulz, M., Guibert, S., Kinne, S., Balkanski, Y., Bauer, S., Berntsen, T., Berglen,
7 T., Boucher, O., Chin, M., Dentener, F., Easter, R., Fillmore, D., Ghan, S., Ginoux, P.,
8 Gong, S., Grini, A., Hendricks, J., Horowitz, L., Huang, P., Isaksen, I., Iversen, T.,
9 Kloster, S., Koch, D., Kirkevåg, A., Kristjansson, J. E., Krol, M., Lauer, A., Lamarque,
10 J., Liu, X., Montanaro, V., Myhre, G., Penner, J., Pitari, G., Reddy, S., Seland, O., Stier,
11 P., Takemura, T., and Tie, X.: Analysis and quantification of the diversities of aerosol
12 life cycles within AeroCom, *Atmos. Chem. Phys.*, 6, 1777–1813, 2006.
- 13 Urbanski, S. P., Salmon, J. M., Nordgren, B. L., and Hao, W. M.: A MODIS direct broadcast
14 algorithm for mapping wildfire burned area in the western United States, *Remote Sens.*
15 *Environ.*, 113, 2511–2526, 2009.
- 16 Waibel, A. E., Fischer, H., Wienhol, F. G., Siegmund, P. C., Lee, B., Ström, J., Lelieveld, J.,
17 and P. J. Crutzen: Highly elevated carbon monoxide concentrations in the upper
18 troposphere and lowermost stratosphere at northern midlatitudes during the STREAM II
19 summer campaign in 1994, *Chemosphere*, 1(1–3), 233–248, 1999.
- 20 Wang, R., Tao, S., Balkanski, Y., Ciais, P., Boucher, O., Liu, J., Piao, S., Shen, H., Vuolo, M.
21 R., Valari, M., Chen, H., Chen, Y., Cozic, A., Huang, Y., Li, B., Li, W., Shen, G.,
22 Wang, B., and Zhang, Y.: Exposure to ambient black carbon derived from a unique
23 inventory and high resolution model, *Proc. Natl. Acad. Sci. U. S. A.*, 14(7), 2459–2463,
24 2014.
- 25 Wang, P. K.: Moisture plumes above thunderstorm anvils and their contributions to cross-
26 tropopause transport of water vapor in midlatitudes, *J. Geophys. Res.*, 108(D6), 4194,
27 2003.
- 28 Wang, Q., Jacob, D. J., Spackman, J. R., Perring, A. E., Schwarz, J. P., Moteki, N., Marais, E.
29 A., Ge, C., Wang, J., and Barrett, S. R. H.: Global budget and radiative forcing of black
30 carbon aerosol: Constraints from pole-to-pole (HIPPO) observations across the Pacific,
31 *J. Geophys. Res. Atmos.*, 119, 2014.
- 32 Warneke, C., Bahreini, R., Brioude, J., Brock, C. A., de Gouw, J. A., Fahey, D. W., Froyd, K.
33 D., Holloway, J. S., Middlebrook, A., Miller, L., Montzka, S., Murphy, D. M., Peischl,
34 J., Ryerson, T. B., Schwarz, J. P., Spackman, J. R., and Veres, P.: Biomass burning in



- 1 Siberia and Kazakhstan as an important source for haze over the Alaskan Arctic in April
2 2008, *Geophys. Res. Lett.*, 36, L02813, 2009.
- 3 Warneke, C., Froyd, K. D., Brioude, J., Bahreini, R., Brock, C. A., Cozic, J., de Gouw, J. A.,
4 Fahey, D. W., Ferrare, R., Holloway, J. S., Middlebrook, A. M., Miller, L., Montzka, S.,
5 Schwarz, J. P., Sodemann, H., Spackman, J. R., and Stohl, A.: An important
6 contribution to springtime Arctic aerosol from biomass burning in Russia, *Geophys.*
7 *Res. Lett.*, 37, L01801, 2010.
- 8 Wotawa, G., and Trainer M.: The influence of Canadian forest fires on pollutant
9 concentrations in the United States, *Science*, 288(5464), 324–328, 2000.
- 10



1 **TABLE CAPTIONS**

2 **Table 1.** List of simulations from this study to characterize the transport and origin of BC.

Name	Anthropogenic sources	BB sources	Purpose
FEI-NE+MACCity	MACCity	FEI-NE	Study of BC transport to the Arctic
MACCity	MACCity	MACCity	Comparison with the combined FEI-NE+MACCity run
Europe	–	FEI-NE	Study of BC originating from Europe by masking this region
Asia	–	FEI-NE	Study of BC originating from Asia by masking this region
Siberia	–	FEI-NE	Study of BC originating from Siberia by masking this region
Kazakhstan	–	FEI-NE	Study of BC originating from Kazakhstan by masking this region
Mongolia	–	FEI-NE	Study of BC originating from Mongolia by masking this region
35°N–40°N (10°W–170°E)	–	FEI-NE	Study of BC originating from latitudes 30°N–40°N in Eurasia by masking this region
40°N–50°N (10°W–170°E)	–	FEI-NE	Study of BC originating from latitudes 40°N–50°N in Eurasia by masking this region
50°N–60°N (10°W–170°E)	–	FEI-NE	Study of BC originating from latitudes 50°N–60°N in Eurasia by masking this region
60°N–90°N (10°W–170°E)	–	FEI-NE	Study of BC originating from latitudes >60°N in Eurasia by masking this region

3
4



1 **Table 2.** Comparison between annual BC emissions (Tg) for the period 2002–2013 (FEI-NE+MACCity) and MACCity emissions for the same
 2 period. The deposition of BC (ktons or kt) from vegetation fires over the Arctic is also compared to those from the MACCity inventory.

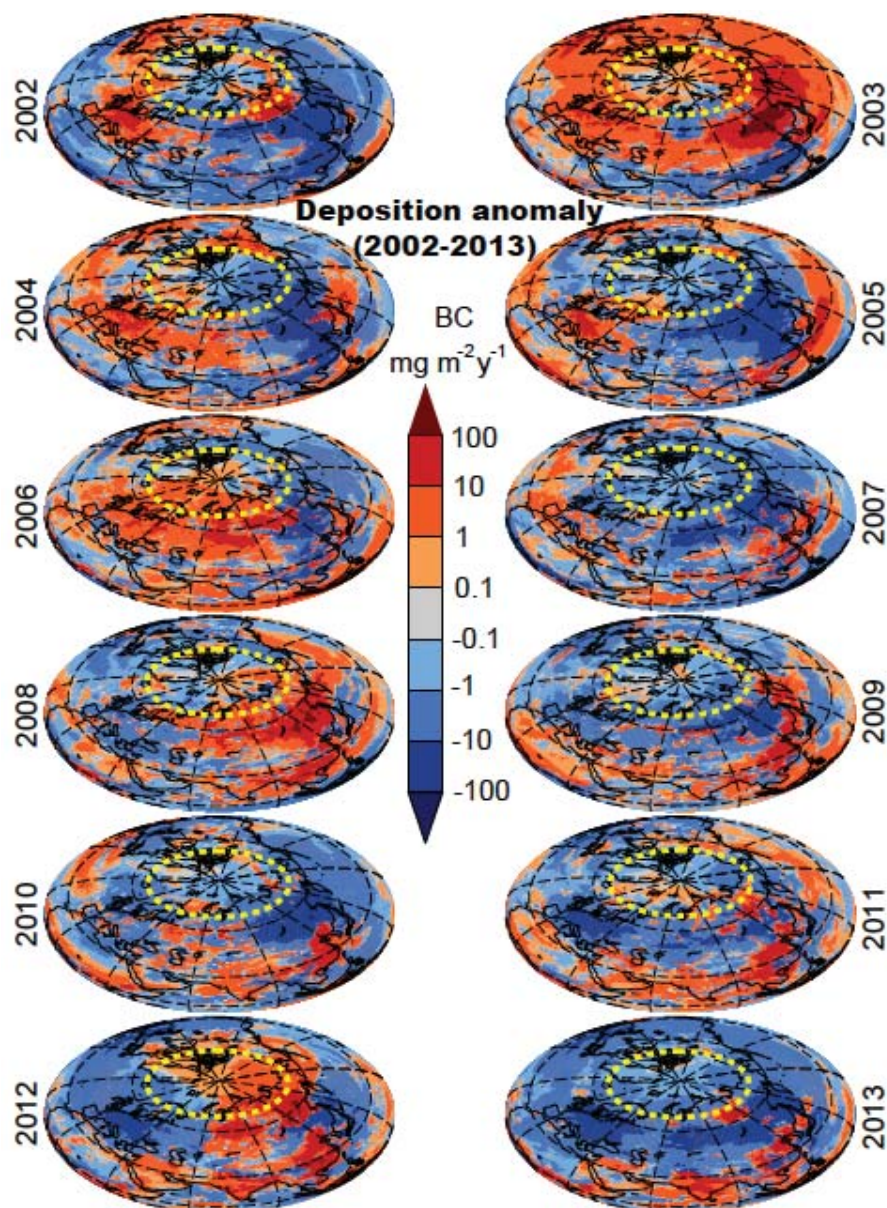
	2002	2003	2004	2005	2006	2007	2008	2009	2010	2011	2012	2013	Range
Anthropogenic sources (Tg)	5.22	5.26	5.30	5.34	5.31	5.28	5.25	5.23	5.20	5.17	5.15	5.15	5.15–5.34
Anthropogenic sources in Eurasia (Tg)	2.26	2.26	2.27	2.28	2.28	2.27	2.26	2.25	2.24	2.23	2.20	2.20	2.20–2.28
BB sources (FEI-NE+MACCity) (Tg)	2.83	4.22	2.98	2.89	3.29	2.74	3.47	3.03	2.82	3.15	3.55	2.90	2.74–4.22
FEI-NE fires in Eurasia (Tg)	0.62	2.19	0.57	0.47	0.90	0.57	1.39	0.69	0.45	0.77	1.17	0.53	0.45–2.19
FEI-NE+MACCity total (Tg)	8.05	9.48	8.28	8.23	8.60	8.02	8.72	8.26	8.02	8.32	8.70	8.05	8.02–9.48
Arctic deposition from fires in Eurasia (kt)	84	98	43	36	88	29	79	42	49	58	120	51	29–120
Arctic deposition from anthropogenic sources (kt)	38	44	38	42	41	36	38	36	33	36	32	28	28–44
Total deposition over the Arctic (kt)	122	142	81	78	129	65	117	78	82	94	152	79	65–152
MACCity anthropogenic sources (Tg)	5.22	5.26	5.30	5.34	5.31	5.28	5.25	5.23	5.20	5.17	5.15	5.15	5.15–5.34
MACCity anthropogenic sources in Eurasia (Tg)	2.26	2.27	2.27	2.28	2.27	2.27	2.26	2.25	2.24	2.22	2.20	2.20	2.20–2.28
MACCity BB sources globally (Tg)	2.51	2.47	2.55	2.57	2.34	2.64	2.04	2.62	2.62	2.62	2.62	2.62	2.04–2.62
MACCity BB (GFED3) in Eurasia (Tg)	0.30	0.43	0.13	0.13	0.21	0.14	0.25	0.24	0.24	0.24	0.24	0.24	0.13–0.43
MACCity total (Tg)	7.73	7.73	7.85	7.91	7.65	7.92	7.29	7.85	7.82	7.79	7.77	7.76	7.29–7.92
Wet deposition over the Arctic (kt)	64	65	50	49	54	40	52	52	51	51	50	42	42–65
Dry deposition over the Arctic (kt)	5	6	6	6	4	3	3	5	5	5	5	4	3–6
Total deposition over the Arctic (kt)	69	71	56	55	58	43	55	57	56	56	55	46	43–71

3
 4



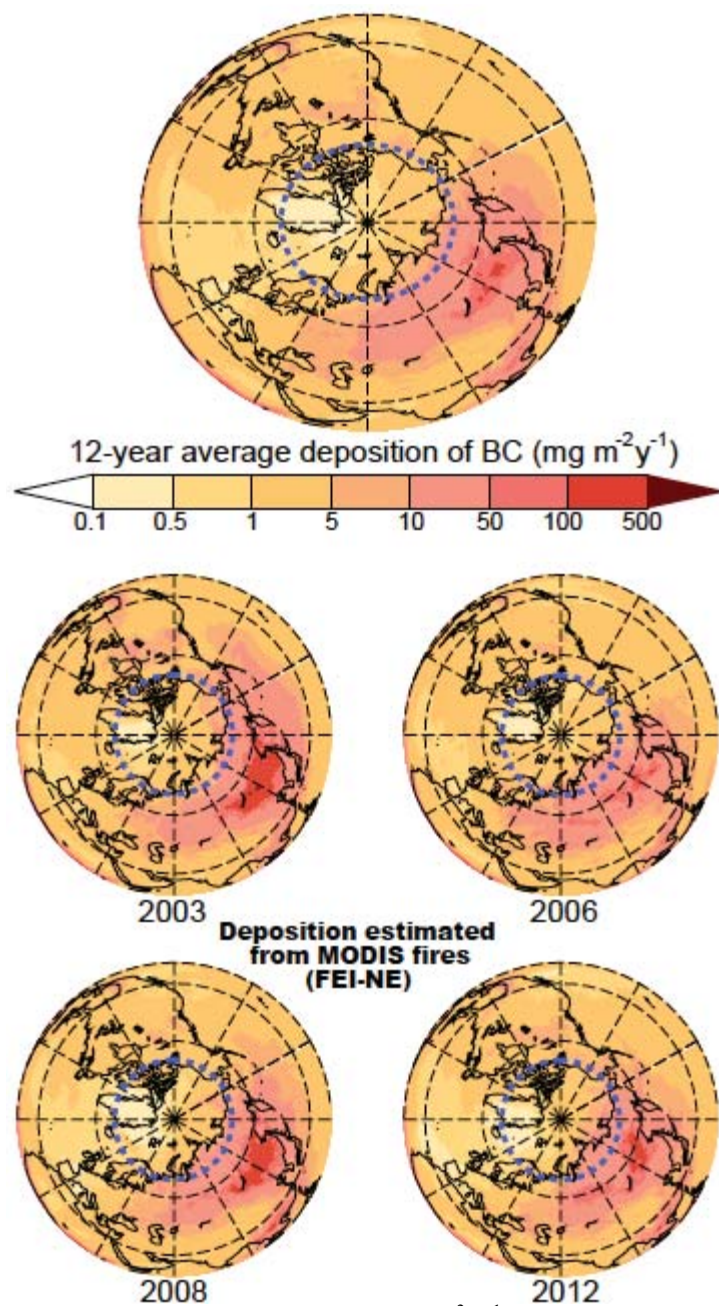
1 **FIGURES**

2

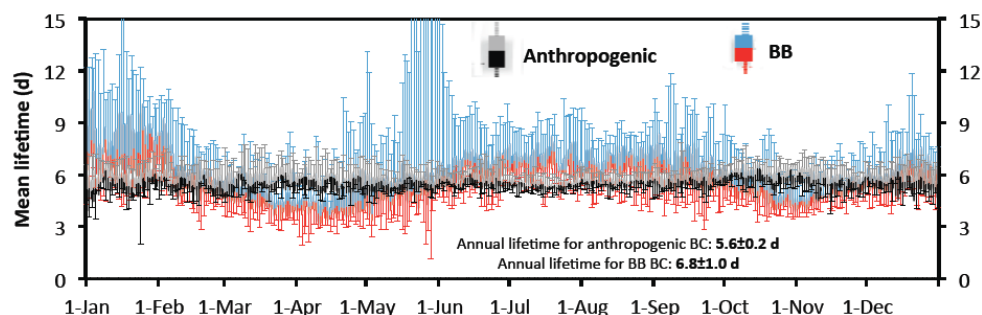


3

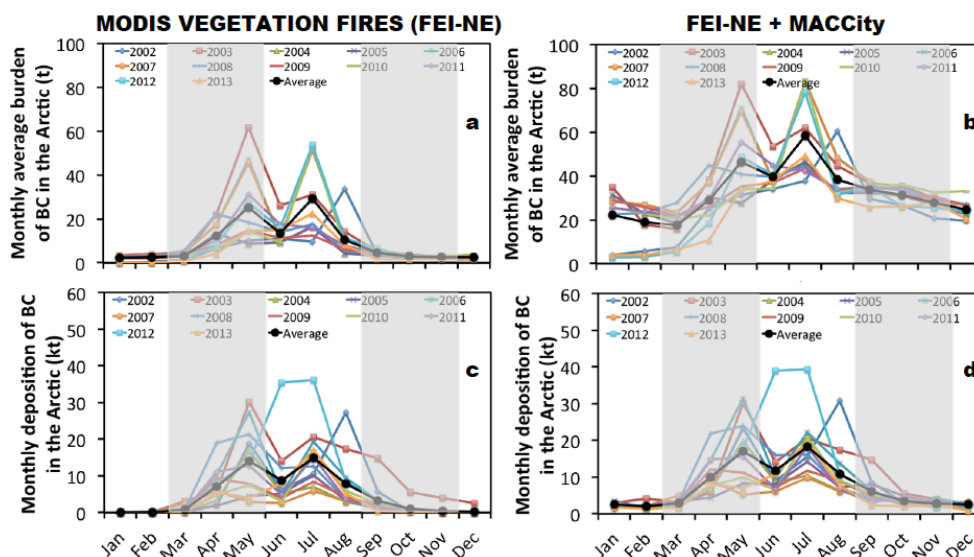
4 **Figure 1.** Deposition anomalies of BC ($\text{mg m}^{-2} \text{y}^{-1}$) in the North Hemisphere for the period
5 2002–2013 from our combined simulation (FEI-NE+MACCity) in Northern Eurasia. The
6 dashed yellow line represents the border of the Arctic ($\sim 67^\circ\text{N}$). Note that the most intense
7 years were estimated to be 2003, 2006, 2008, and 2012.



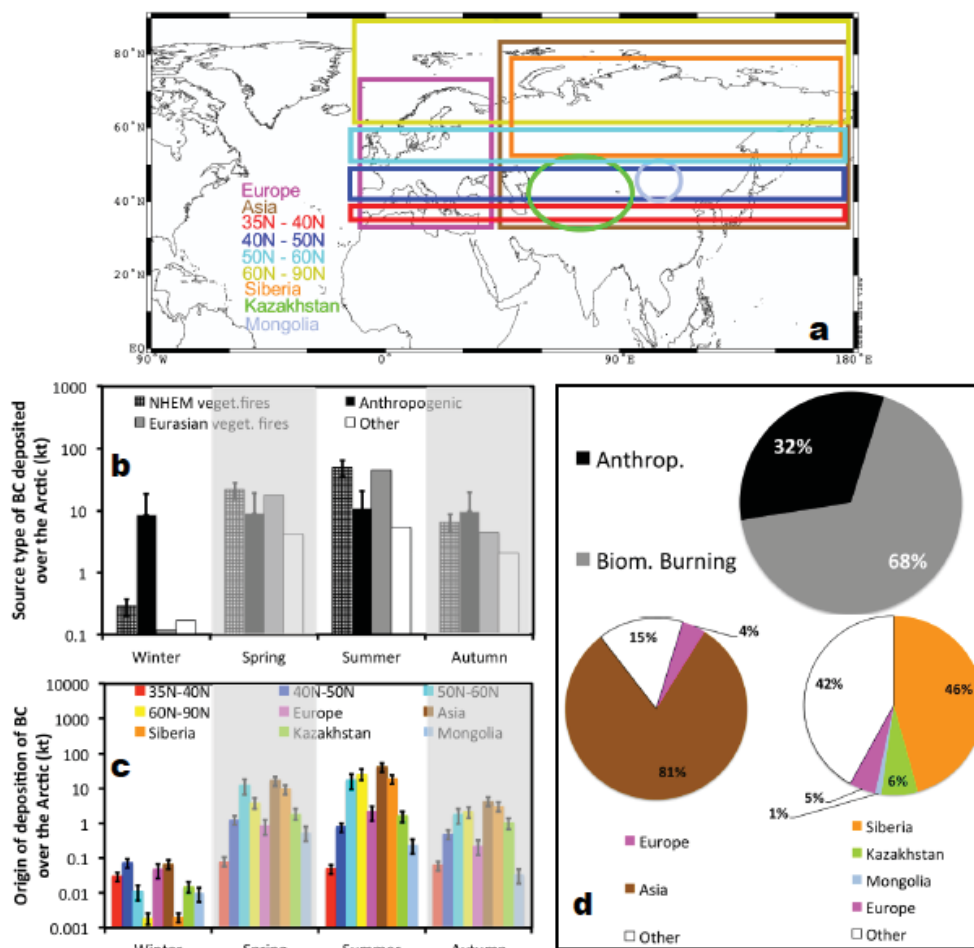
1
2 **Figure 2.** Arctic deposition of BC ($\text{mg m}^{-2} \text{y}^{-1}$) from BB emission according to the FEI-NE
3 inventory. The upper panel depicts the 12-year average deposition, while the lower 4 panels
4 show the most intense fire years (2003, 2006, 2008, and 2012). The dashed blue line
5 represents the border of the Arctic ($\sim 67^\circ\text{N}$).



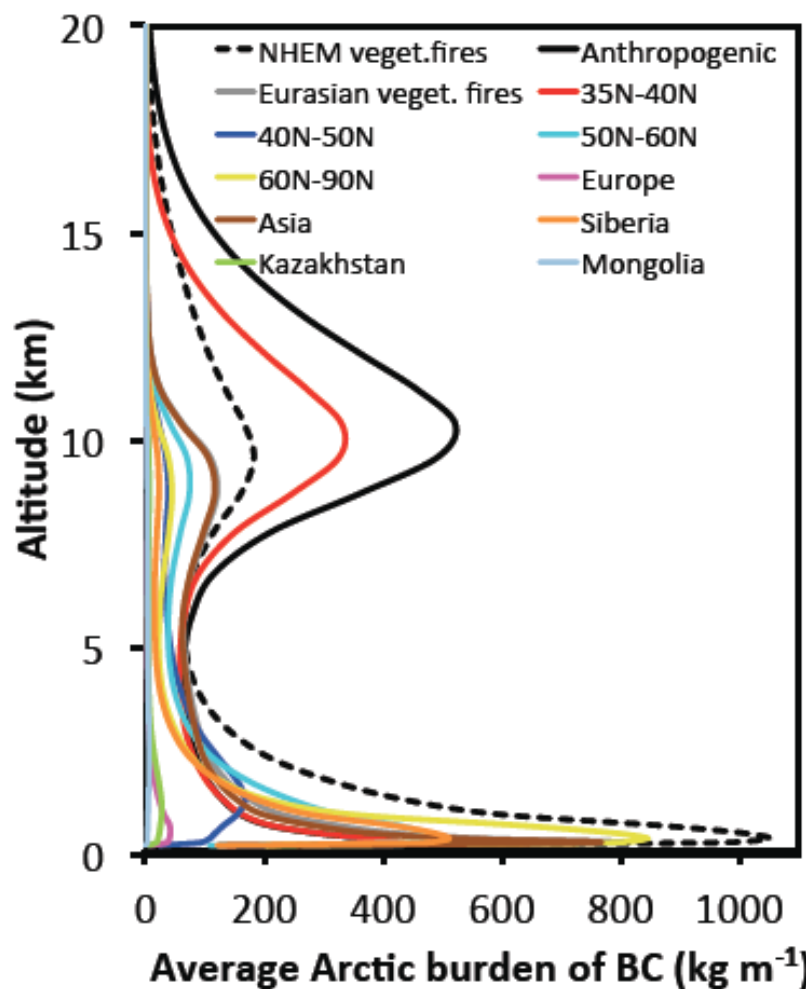
1 1-Jan 1-Feb 1-Mar 1-Apr 1-May 1-Jun 1-Jul 1-Aug 1-Sep 1-Oct 1-Nov 1-Dec
 2 **Figure 3.** Annual mean lifetime of the global anthropogenic and BB BC from our combined
 3 FEI-NE+MACCity simulation. The results are presented as Box & Whisker plots of daily
 4 lifetimes of BC (both for anthropogenic and BB) for the period 2002–2013. The plot shows
 5 the minimum value, the 25th percentile, which holds 25% of the values at or below it. The
 6 median is the 50th percentile, the third quartile is the 75th percentile and the maximum is the
 7 100th percentile (i.e., 100% of the values are at or below it).



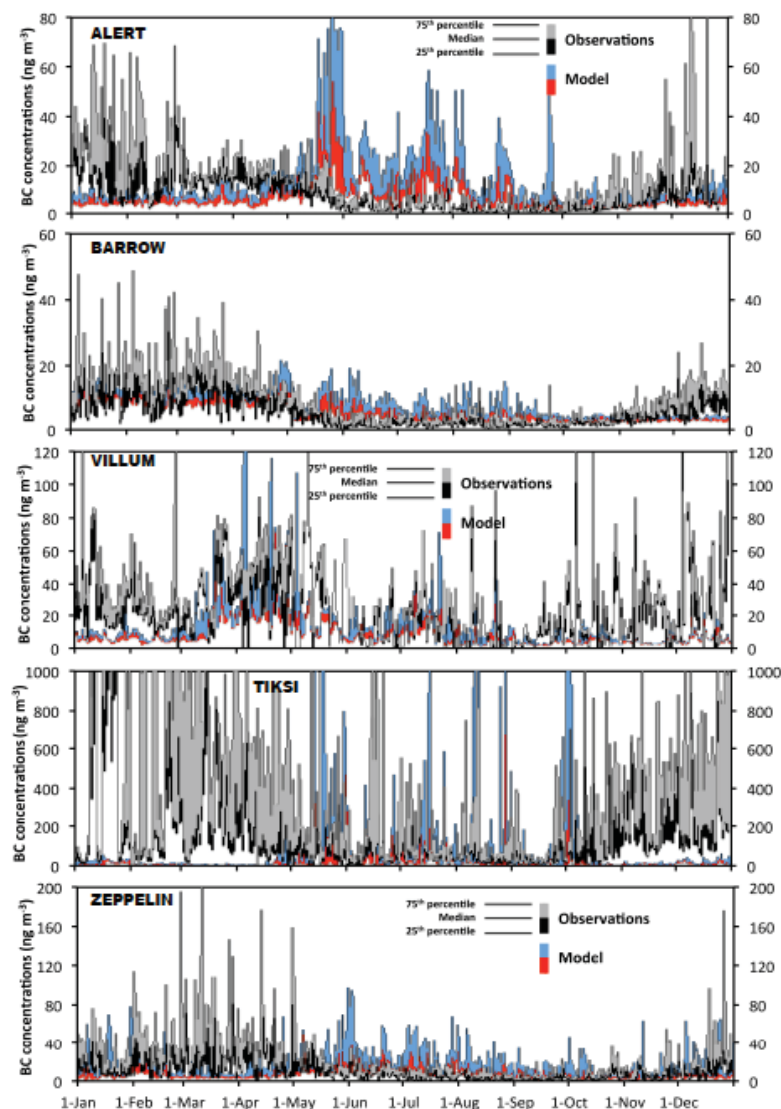
8
 9 **Figure 4.** Monthly atmospheric burden of BC (t) in the Arctic with each year between 2002
 10 and 2013 represented by a different colored line: (a) from vegetation fires (FEI-NE) only and
 11 (b) from all BC emissions (FEI-NE+MACCity). Panel c and d shows the same, but for the
 12 Arctic deposition of BC (kt).



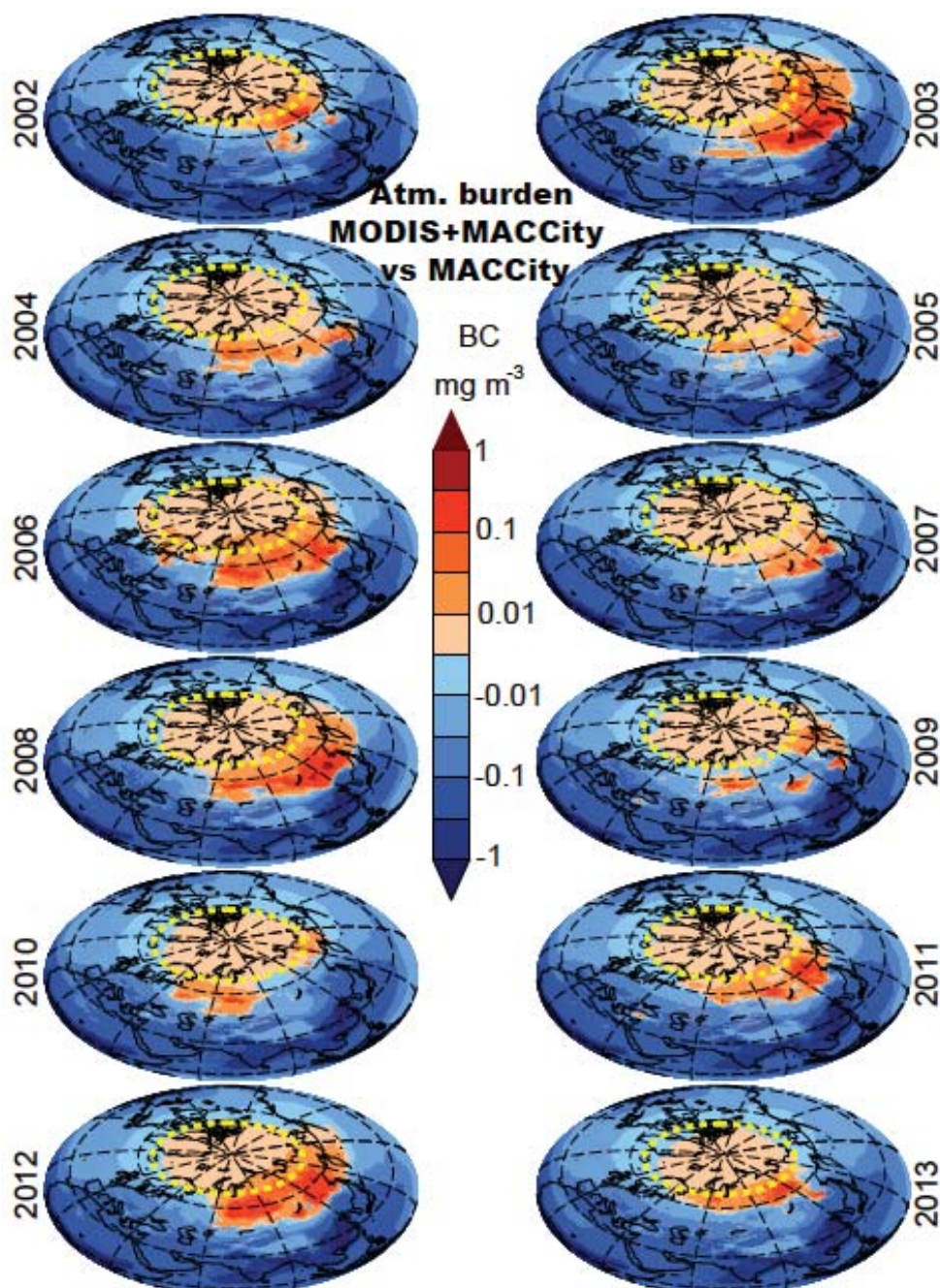
1
 2 **Figure 5.** (a) The nine geographic regions of BC emission in Northern Eurasia defined for
 3 this study. (b) Seasonal values of BC emitted from all fires in Northern Hemisphere (NHEM),
 4 anthropogenic sources (black) and Northern Eurasian vegetation fires (grey) deposited in the
 5 Arctic for the period of 2002–2013. (c) Contribution of several geographic regions to the
 6 Arctic BC deposition. Colors are used according to the ones used in panel a. Red stands for
 7 regions within 35°N–40°N, dark blue for 40°N–50°N, turquoise for 50°N–60°N, yellow for
 8 regions located above 60°N (60°N–90°N), magenta for Europe, brown for Asia, orange
 9 denotes Siberia, green for Kazakhstan, and light blue for Mongolia. (d) Pie-charts showing
 10 the origin of BC deposition in the Arctic from vegetation fires in Northern Eurasia.



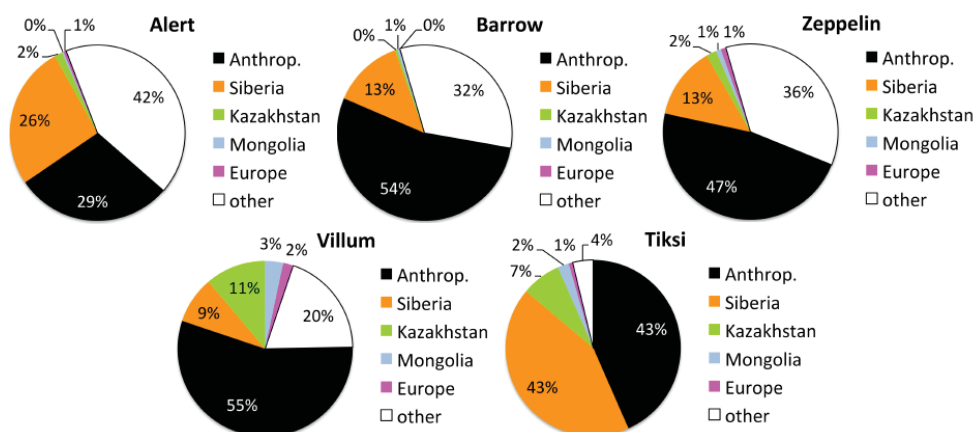
1
2 **Figure 6.** Annual average (2002–2013) vertical profiles of atmospheric burden of BC (kg m^{-3})
3 ¹⁾ in the Arctic originating from different regions.



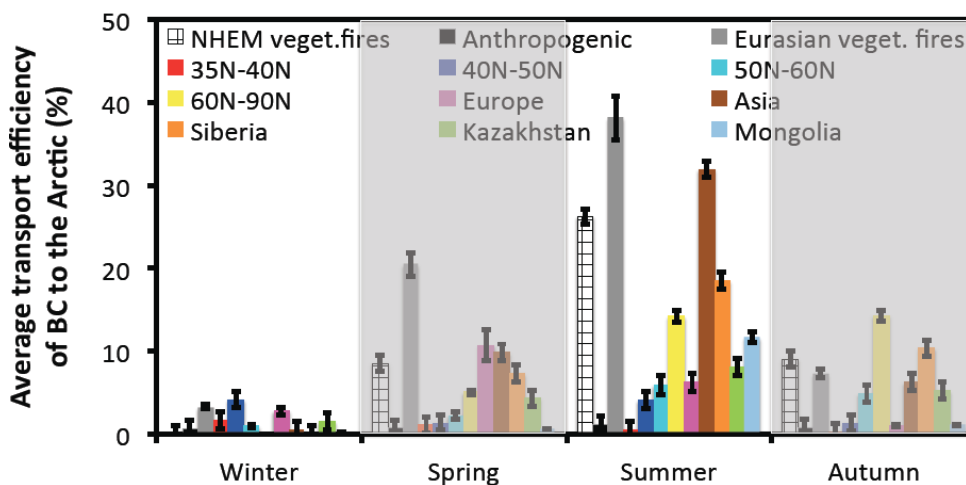
1
2 **Figure 7.** Modeled versus measured surface concentrations of BC (ng m^{-3}) for the FEI-
3 NE+MACCity simulation in the Arctic stations Alert, Barrow, Villum, Tiksi, and Zeppelin.
4 Due to the high variability of the surface concentrations, the results are presented as Box &
5 Whisker plots of all the modeled and measured surface daily concentrations of BC for the
6 period 2002–2013. The plots show the minimum value, the 25th percentile, which holds 25%
7 of the values at or below it. The median is the 50th percentile, the third quartile is the 75th
8 percentile and the maximum is the 100th percentile (i.e., 100% of the values are at or below
9 it).



1
2 **Figure 8.** Difference in BC atmospheric burden (mg m^{-3}) between our simulation that
3 combines emission inventories (FEI-NE+MACCity) and MACCity. The dashed yellow line
4 represents the limit of the Arctic ($\sim 67^\circ\text{N}$). The BC burden was estimated by averaging all the
5 vertical layers over 365 days for each year from 2002 to 2013.



1
 2 **Figure 9.** Multi-year average (2002–2013) contribution of global anthropogenic and BB BC
 3 from the respective geographic regions to surface concentrations at the Arctic stations (Alert,
 4 Barrow, Zeppelin, Villum, and Tiksi). “Other” stands for other locations where BB sources
 5 were not accounted for.



6
 7 **Figure 10.** Relative transport efficiency of BC from vegetation fires from different
 8 geographic regions across the Arctic. The same colors were used as in **Figure 5**.

9